Elucidating female-specific differentiation genes in the mosquito, *Aedes aegypti*

by

Daniel Heschuk

A thesis submitted to the Faculty of Graduate Studies of the University of Manitoba

in partial fulfillment of the requirements of the degree of:

Master of Science

Department of Biological Sciences

University of Manitoba

Winnipeg, Manitoba, Canada

ABSTRACT

Insects account for the vast majority of sexually reproducing animals described and demonstrate significant diversity and complexity in sex-developmental pathways. While only a small number of insect species have had sex-development pathways characterized, orthologues of the master regulator of sex-differentiation, *Doublesex (Dsx)*, have been identified in all insects studied. Using alternative splicing to produce distinct, functional male-specific and female-specific isoforms, Dsx guides differential gene expression patterns through its activity as a transcription factor. Notably, while male and female specific isoforms contain identical DNA-binding domains, it is expected that sex-specific differences in gene expression are the result of different binding partners at the isoform specific oligomerization domains.

The yellow fever mosquito, *Aedes aegypti*, exhibits pronounced sexual dimorphisms, largely due to the females' specific need to obtain blood meals. Because of these distinct dimorphic features and its threat to human health, research into *Ae. aegypti* sex development is of interest to developmental biologists and in the context of public health. Despite numerous studies on *Ae. aegypti* sex development, little is known about the isoform-specific binding partners of *AaeDsx*. Using protein pulldown and mass spectrometry techniques, this project examined the distinct binding partners of the two female-specific DSX isoforms with the specific aims of improving our understanding of insect sex development and discovering new gene targets for female lethality. A subset of 12 genes identified in the mass spectrometry assay were further subjected to RNA interference assays where female-specific developmental impacts were assessed. Data from this project may be applied to improve sex-sorting of mosquitoes in sterile insect technique approaches.

ACKNOWLEDGEMENTS

First and foremost, thank you, Dr. Steve Whyard, for your guidance, support, and perfectly timed dad jokes. These past 5 years in the Whyard Lab have been a pleasure and have provided experiences and opportunities that were truly invaluable. I am beyond grateful for everything you've done for me, all the times you've looked out for me, and every opportunity you've recommended to me with the knowledge that it would help me succeed.

I must also thank my committee members Dr. Gerd Prehna and Dr. Olivia Wilkins. Both of whom provided expert guidance and feedback, alongside excellent (sometimes tangential, but always engaging) conversations. I must also thank Dr. Prehna and the members of his lab for their help and equipment use during my protein expression. Here, I'll have to give a big thank you to Matthew Van Schepdael, my roommate and Prehna Lab confidant, for always offering his help and guidance at the drop of a hat.

Finally, thank you to all members of the Whyard Lab, both past and present. Over the years this lab has changed significantly with numerous people coming and going, but it always has remained a fantastic place to work, and I am especially grateful to everyone I have worked with. Thank you especially to Alison Tayler and Aditi Singh, both of whom have been excellent mentors during my time here and have provided exceptional help and guidance during my projects. Thank you also to Michael Wood, Elizabeth Jonson, Nazanin Amanat, and Chris Manchur for being amazing peers to work with, play croquet against, and grab coffee with.

TABLE OF CONTENTS

ABSTRACT ..... **ii**

ACKNOWLEDGEMENTS ..... **iii**

LIST OF TABLES ..... **vi**

LIST OF FIGURES ..... **vii**

LIST OF ABBREVIATIONS ..... **viii**

1 INTRODUCTION **9**

1.1 Insect sex-development **9**

1.1.1 Overview and significance 9

1.1.2 A cytogenetic basis for sex-determination in insects 10

1.1.3 Genes involved in insect sex-determination 11

1.1.4 Doublesex and Sex-Differentiation 14

1.2 Sexual dimorphisms in the mosquito, Aedes aegypti **16**

1.2.1 Overview of Aedes aegypti 16

1.2.2 Differentially expressed transcripts 19

1.2.3 Dimorphic anatomies, behaviours, and physiologies 21

1.3 Applications in Insect Control **24**

1.3.1 Selecting for male-only populations 24

1.4 Research Objectives **25**

1.3.1 OBJECTIVE 1: Compare expression levels and binding partners of DSX^{F1} and DSX^{F2} 26

1.3.2 OBJECTIVE 2: Identify DSX^{F}-interacting proteins essential for female development 26

2 MATERIALS AND METHODS **27**

2.1 Rearing of Insects **27**

2.2 Isolation of RNA and cDNA Synthesis **27**

2.3 Sex-sorting of Aedes aegypti **28**

2.4 Quantitative Reverse Transcriptase PCR (qRT-PCR) Analysis **29**

2.5 Expression of His-tagged Doublesex Proteins and GST-tagged Binding Partners 29

2.6 Large Scale Induction and Purification of Fusion Proteins **31**

2.7 Purification of His-tagged proteins **32**

2.8 Purification of GST-tagged proteins **33**

2.9 Size Exclusion Chromatography **34**

2.10 Aedes aegypti nuclear extractions **34**

2.11 Nuclear Protein Pulldowns and Mass Spectrometry **35**

2.12 Confirmation of Mass Spectrometry Analysis using GST-Pulldowns 35
2.13 Bacterial dsRNA Expression 36
2.14 Bacterial Feeding of dsRNA to Mosquito Larvae 38
2.15 Sex-biased protein expression analysis 38
3 RESULTS 39
3.1 Isoform specific expression of Dsx transcripts across larval and pupal development 39
3.2 Expression of Recombinant DSX Proteins 40
3.3 Prospective DSX^F Binding Partners Determined in Mass Spectrometry Analysis 43
3.4 Expression of Recombinant Proteins for DSX Pulldown Assays 44
3.5 Confirmation of DSX^{F1} and $DSXF^2$ Binding Interactions through Protein Pulldowns 46
3.6 Impacts on mosquito development following consumption of bacterial dsRNA .. 47
3.7 Impact of temperature on dsRNA treatments 52
3.8 Sex-biased protein expression 54
4 DISCUSSION 56
4.1 Comparisons between DSX^{F1} and DSX^{F2} 56
4.2 Identification of new targets for female-specific development 58
4.3 Applications and optimization of female-specific developmental delay 61
5 CONCLUSIONS AND FUTURE DIRECTIONS 64
6 REFERENCES 66
7 APPENDIX 74

LIST OF TABLES

Table 1. Selection criteria for 12 gene targets identified in mass spectrometry analysis……..44

Table 2. Summary of dsRNA feeding assay data 49

Table A1. Primers used for this study..... 74

Table A2. Coding sequences for recombinant proteins 76

Table A3. Identified DSX^{F1} / DSX^{F2} binding partners from mass spectrometry analysis..... 78

Table A4. DsRNA sequences 81

LIST OF FIGURES

Figure 1. Sex-determination pathway in *Aedes aegypti*..... 17

Figure 2. Protein sequence alignment comparing *Ae. aegypti* and *D. melanogaster* Doublesex. 18

Figure 3. Sexual dimorphisms in *Aedes aegypti*..... 23

Figure 4. Expression of Dsx^{F1} and Dsx^{F2} during mosquito development..... 39

Figure 5. Sex-limited expression of *Doublesex* isoforms in *Aedes aegypti*..... 40

Figure 6. Small scale bacterial expression of 6xHis-tagged DSX^{F1} and DSX^{F2} proteins..... 41

Figure 7. Detection of His-tagged Doublesex following nickel column purification..... 41

Figure 8. FPLC purification of 6xHis-tagged DSX^{F1} and DSX^{F2} proteins..... 42

Figure 9. Large scale purification of GST-tagged DSX^{F} binding partners..... 45

Figure 10. Pulldown of His-tagged DSX^{F1} and DSX^{F2} 47

Figure 11. Interval between male and female eclosion is impacted by the consumption of various dsRNAs targeting genes identified in mass spectrometry 50

Figure 12. Altered female development following consumption of dsRNA targeting transcripts from mass-spectrometry analysis..... 51

Figure 13. Impact of temperature on dsRNA treatments and male-female pupation interval..... 53

Figure 14. Impact of temperature and dsRNA treatments on pupation timing..... 54

Figure 15. Sex-biased protein expression 55

LIST OF ABBREVIATIONS

ChIP	Chromatin Immunoprecipitation
DET	Differentially expressed transcript
dsRNA	Double-stranded RNA
DSX	Doublesex
DTT	Dithiothreitol
EDTA	Ethylenediaminetetraacetic acid
FPLC	Fast protein liquid chromatography
Fru	Fruitless
GST	Glutathione S-transferase
IPTG	Isopropyl β-D-1-thiogalactopyranoside
LB	Lysogeny broth
PAGE	Polyacrylamide gel electrophoresis
PCR	Polymerase chain reaction
PMSF	Phenylmethylsulfonyl fluoride
RNAi	RNA interference
Rpb8	DNA-directed RNA-polymerase subunit rpb8
SDS	Sodium dodecyl sulfate
SIT	Sterile insect technique
SXL	Sex-lethal
Tra	Transformer
WD48	WD-repeat containing protein 48 homolog
XSE	X-linked signal element

1 INTRODUCTION

1.1 Insect sex-development

1.1.1 Overview and significance

Early development in sexually-reproducing, gonochoristic animals is defined by a decision between following a male or female pathway of development. Sex-specific developmental programs are complex, and lead to sex-specific morphological, physiological, and behavioural differences in the adult form (Biedler and Tu, 2016; Blackmon et al., 2017). Insects account for 81.3% of all animals described, and hence, present a comparatively large diversity of sex-determination and differentiation pathways, even amongst closely related species (Biedler and Tu, 2016; Krzywinska et al., 2016; Scudder, 2009; Verhulst et al., 2010). Cytogenetic studies have identified the general mechanisms of sex-determination in numerous insect species and helped identify some of the key sex-determination genes in many insects (Blackmon et al., 2017), but the diversity of specific genes and pathways involved in sex differentiation are largely undefined. One of the best-understood sex-development pathways comes from the model organism, *Drosophila melanogaster* (Kopp, 2012; Price et al., 2015a; Salz and Erickson, 2010). Despite this in-depth understanding of one sex-development pathway, studies in other insects have demonstrated significant deviations from the canonical pathway observed in *D. melanogaster* (Biedler and Tu, 2016; Blackmon et al., 2017; Cho et al., 2007; De La Filia et al., 2015; Dübendorfer et al., 2002; Price et al., 2015a). While closely related insects can demonstrate similar developmental programs, only an in-depth genetic analysis can confirm the sex-development program of any individual species. In all sexually dimorphic organisms,

however, sex-development begins with an initial signal specifying male or female development (Blackmon et al., 2017).

1.1.2 A cytogenetic basis for sex-determination in insects

The development of sexually dimorphic features begins with an initial specification of male or female development, known as sex-determination. Insect sex-determination is primarily a genotypic phenomenon, whereas temperature-dependent, environmental sex-determination has been identified in a small minority of insect species (Blackmon et al., 2017). Within genotypic sex-determination, two general strategies are used: (1) heterogamety; and (2) haplodiploidy (Blackmon et al., 2017; De La Filia et al., 2015). Heterogametic systems may depend on the presence of dominant sex-determination genes, or the ratio of autosomes to X-chromosomes (such is the case in the vinegar fly, *Drosophila melanogaster*) (Blackmon et al., 2017). These systems are further categorized based on which sex produces the sex-determining gametes. In male heterogamety, males are generally classified as "XY" or "XO" individuals, and females, "XX" (Blackmon et al., 2017). In this case, males, but not females can differentially generate gametes which specify the sex of progeny. The opposite is true in female-heterogamety, a far less common method used primarily in lepidopterans and some tephritids, where males are generally represented as "ZZ" and females "ZW" or "ZO" (Blackmon et al., 2017).

The other strategy of genotypic sex-determination is haplodiploidy, where haploid individuals develop into males and diploid individuals develop as females (De La Filia et al., 2015). Haploid individuals may develop from unfertilized eggs (e.g. bees, wasps, ants), or from post-fertilization elimination of the paternal genome (e.g. scale insects) (De La Filia et al., 2015; Gardner and Ross, 2014). The general mechanisms surrounding sex-determination in a

haplodiploid system may involve processes known as complementary sex determination or imprinting (De La Filia et al., 2015; Verhulst et al., 2010). In complementary sex determination, sex is determined based on the complementarity of alleles at a highly variable, sex-determining locus (De La Filia et al., 2015). Female development is specified based on heterozygosity at this locus, whereas males may develop from a hemizygous or homozygous (diploid) condition (Blackmon et al., 2017; De La Filia et al., 2015). Paternal imprinting is a lesser-known mechanism whereby female development relies on a paternally imprinted chromosome, whereas unfertilized eggs can only develop as males (Verhulst, 2010).

Even within the same family, differences in sex-determination may be observed. The chromosomal basis for sex-determination between anopheline (*Anopheles sp.*) and culicine (*Aedes sp.* and *Culex sp.*) mosquitoes, are distinct. Whereas anopheline mosquitoes (XX / XY) have heteromorphic sex-chromosomes, culicine mosquitoes use an autosomal, non-recombining, sex-determining locus (Biedler and Tu, 2016; Krzywinska et al., 2016). Significantly, this means that anopheline mosquitoes must have a dosage-compensation mechanism to account for differences in X-linked gene expression, whereas culicine mosquitoes do not (Krzywinska et al., 2021, 2016; Rose et al., 2016). In the malaria vector, *Anopheles gambiae*, dosage compensation relies on the hyperactivation of genes on the singular male X-chromosome (Rose et al., 2016). In the absence of the male-determining gene, *Yob*, the female-specific gene, *femaleless*, is expressed and prevents hyperactivation of X-linked gene expression(Krzywinska et al., 2021).

1.1.3 Genes involved in insect sex-determination

In only a small subset of insects have the specific genetic repertoires surrounding sex-determination been comprehensively researched. The best-characterized sex-determination

pathway is of the model organism, *Drosophila melanogaster* (Salz and Erickson, 2010). While the molecular pathways guiding sex-determination and differentiation are diverse, what has been learned from *D. melanogaster* has guided our understanding of sex-development across metazoans.

In *D. melanogaster*, an 'X-counting' mechanism provides the basis for sex-determination (Salz and Erickson, 2010). Female development requires sufficient expression of four genes (*Runt*, *Scute*, *SisA*, and *Unpaired*) encoded on the X-chromosome, known collectively as X-linked signal elements (XSE) (Salz and Erickson, 2010). Through their binding to an early promoter, XSEs function to initiate an autoregulatory cycle of a protein known as 'sex-lethal' (SXL). SXL is an RNA-binding protein that notably acts to direct its own splicing, producing functional *sxl* mRNA even after XSE gene expression diminishes (Penalva and Sánchez, 2003; Salz and Erickson, 2010). In males, where only one X-chromosome is present and XSE-expression is low, *sxl* is still expressed through its "maintenance promoter" (Salz and Erikson, 2010). However, without sufficient XSE expression, the default splicing pattern of *sxl* yields an early stop codon, resulting in a truncated, non-functional Sxl protein (Salz and Erickson, 2010).

Functional Sxl found in female *D. melanogaster* acts to guide the sex-specific splicing of a gene known as *"transformer"* (*tra*) (Penalva and Sánchez, 2003; Verhulst et al., 2010). Similarly, only the female-specific splice-pattern of *tra* mRNA yields a functional Tra protein, excluding an exon with a premature stop codon found in the male isoform (Verhulst et al., 2010). Functional Tra then acts in combination with the non-sex-specific Transformer 2 (Tra2) to guide the female-specific splicing of two genes, *Doublesex* (*dsx*), and *Fruitless* (*fru*) (Salz and Erickson, 2010). While only the male splice variant of *fru* yields a functional protein which governs male-specific mating behaviours, both male and female *dsx* variants code for functional

Dsx protein to give their distinct, sex-specific isoforms, Dsx^M and Dsx^F, respectively (Salz and Erickson, 2010). Acting at the end of the sex-determination pathway, Dsx acts as a master regulator of sex-differentiation, bridging the gap between sex-determination and differentiation (Cho et al., 2007; Clough et al., 2014; Ledón-Rettig et al., 2017; Salvemini et al., 2011; Shukla and Palli, 2012).

Doublesex appears to have a well-conserved function and orthologues have been found in all insects studied to date (Cho et al., 2007; Ledón-Rettig et al., 2017). Comparatively, the upstream effectors of *Dsx* are divergent and exhibit rapid evolution (Biedler and Tu, 2016; Salz and Erickson, 2010). Not only does this mean that there is significant variability in the genetic pathways acting upstream to specify the male or female-splicing of *Dsx*, but there is also variability in which Dsx isoform is spliced by default (Biedler and Tu, 2016). For example, insects such as the honeybee (*Apis mellifera*), the silk moth (*Bombyx mori*), and *D. melanogaster* undergo male development in the absence of a feminizing factor (Beye et al., 2003; Kiuchi et al., 2014; Salz and Erickson, 2010). In contrast, insects like the red flour beetle (*Tribolium castaneum*) and the housefly (*Musca domestica*) use male-factors (M-factors) as their primary sex-determination signal and, in their absence, female-specific splicing of Dsx results (Dübendorfer et al., 2002; Shukla and Palli, 2012). *Ae. aegypti* and *An. gambiae* mosquitoes rely on the dominant M-factors *Nix* and *Yob*, respectively, to counter the default female splicing of Dsx (Aryan et al., 2020; Krzywinska et al., 2016; Liu et al., 2020).

Studies of the mosquito *Ae. aegypti* and its relative *Ae. albopictus* determined that *Nix* is necessary and sufficient to direct male development (Aryan et al., 2020; Hall et al., 2015; Liu et al., 2020). That is, RNAi-mediated knockdown or CRISPR-mediated silencing of this M-factor led to feminization of genotypically male individuals, whereas ectopic expression of *Nix* in

females produced masculinized individuals (Aryan et al., 2020; Hall et al., 2015; Liu et al., 2020). Nix appears to be a distant homologue of Tra2 and is believed to direct the male-specific splicing of *Dsx*, however its precise mechanism has yet to be determined (Aryan et al., 2020; Hall et al., 2015; Liu et al., 2020). It is possible, however, that Nix functions through partially conserved Tra/Tra2 binding sites found in *Dsx.*

1.1.4 Doublesex and Sex-Differentiation

While sex-determination is the process by which male or female development is specified, sex-differentiation is defined by the development of sex-specific phenotypes in certain tissues and cells. As the master regulator of sex-differentiation, Dsx acts as a transcription factor to guide sex-specific development (Clough et al., 2014; Ledón-Rettig et al., 2017; Salvemini et al., 2011). Notably, Dsx^M and Dsx^F isoforms share similar DNA-binding domains but have distinct C-termini that are believed to differentially bind cofactors that lead to their sex-specific transcription factor activity (Clough et al., 2014). The differential gene-activating or repressing activity of male and female isoforms results in sexually dimorphic gene expression (Ledón-Rettig et al., 2017). Assessing the activity of both Dsx isoforms is challenging as Dsx may also modulate the expression of other transcription factors, thereby indirectly influencing gene expression (Ledón-Rettig et al., 2017). Furthermore, as not all tissues are equally sexually dimorphic, Dsx activity can vary greatly depending on cell type and timing of development (Ledón-Rettig et al., 2017; Rice et al., 2019).

In a study conducted by Clough et al. (2014), chromatin immunoprecipitation followed by sequencing (ChIP-seq) was employed to determine the sex- and tissue-specific binding of Dsx to various genes of *D. melanogaster*. The genes primarily targeted by Dsx represented signalling pathways and transcription factors, implying that Dsx can indirectly impact the expression of

many genes (Clough et al., 2014). Furthermore, very few cases of sex- or tissue-specific occupancy of the Dsx isoforms to their targets were identified, implying that Dsx activity depends primarily on the combinatorial activity of gene- and tissue-specific factors (Clough et al., 2014). This largely unbiased occupancy of the Dsx isoforms to DNA targets suggests that Dsx must coordinate with other sex-, tissue-, or condition-specific factors to mediate the sex-specific differences in gene expression.

Whereas the sex-specific transcription factor activity of DSX is essential for sexually-dimorphic structures to develop, its ectopic activity can be detrimental (Rice et al., 2019). The spatiotemporal, cell-specific control of *dsx* expression in *D. melanogaster* was investigated by Rice et al. (2019), who determined that the transcription of *dsx* is regulated by a series of modular, tissue-specific enhancers. Using pPTGAL GAL4 reporter lines, the authors identified 3 enhancer sequences specific to the *D. melanogaster* foreleg – a structure that contains multiple sexually-dimorphic tissues (Rice et al., 2019). While one of the three regulatory sequences was found to drive broad expression throughout the foreleg, the other two enhancers' activity were restricted to a subset of mutually-exclusive cell-types comprising the sex-comb or sex-specific chemosensory bristles (Rice et al., 2019). The authors suggest that this pattern of modular *dsx* enhancers contributes to precise spatiotemporal *dsx* expression where multiple enhancers can act successively or simultaneously in a tissue and cell-type specific manner.

Because of the complexities surrounding sex- and tissue-specific Dsx activity, multiple techniques may be required to understand the direct and indirect effects of this transcription factor. On their own, techniques such as consensus sequence searches, ChIP sequencing, protein co-immunoprecipitation, RNAi-mediated Dsx-knockdown, and RNA-sequencing methods provide limited information. Thus, the enigmatic nature of Dsx's direct and indirect activity

requires a multifaceted approach to appropriately characterize its target effects. Complicating the issue are the downstream impacts of direct targets of Dsx, whereby many also act as transcription factors with their own target repertoires (Ledón-Rettig et al., 2017; Tomchaney et al., 2014). Furthermore, the sex-specific isoforms of Dsx may act to modulate gene expression in antagonizing ways, or one isoform may influence the expression of a particular gene while the other isoform has no impact (Ledón-Rettig et al., 2017). This process of sex-differentiation, with the tightly regulated molecular programs involved, ultimately leads to sexually dimorphic gene expression patterns, as observed in the yellow fever vector, *Aedes aegypti*.

1.2 Sexual dimorphisms in the mosquito, Aedes aegypti

1.2.1 Overview of Aedes aegypti

Male and female mosquitoes are often noted for their clear anatomical, behavioural, and physiological differences, making them excellent organisms for studying the development of sexual dimorphisms (Biedler and Tu, 2016). As the only sex that blood-feeds, female mosquitoes have antennae equipped with unique odorant receptors to find prey, a skin-piercing proboscis for blood-feeding, and a gut capable of digesting bloodmeals (Lehane, 2005). Significantly, this means that the transmission of mosquito-borne infections is a sex-specific phenomenon. The tropical mosquito, *Aedes aegypti*, is responsible for transmitting diseases such as dengue, Zika, and yellow fever, and current methods of their control can be chemically intensive and harmful to environmental, ecological, and human health (Sanchez-Bayo et al., 2013; Whyard et al., 2015). Understanding the genetic programs responsible for female development may assist in the development of safer population control alternatives, such as the sterile insect technique (Lutrat et al., 2019).

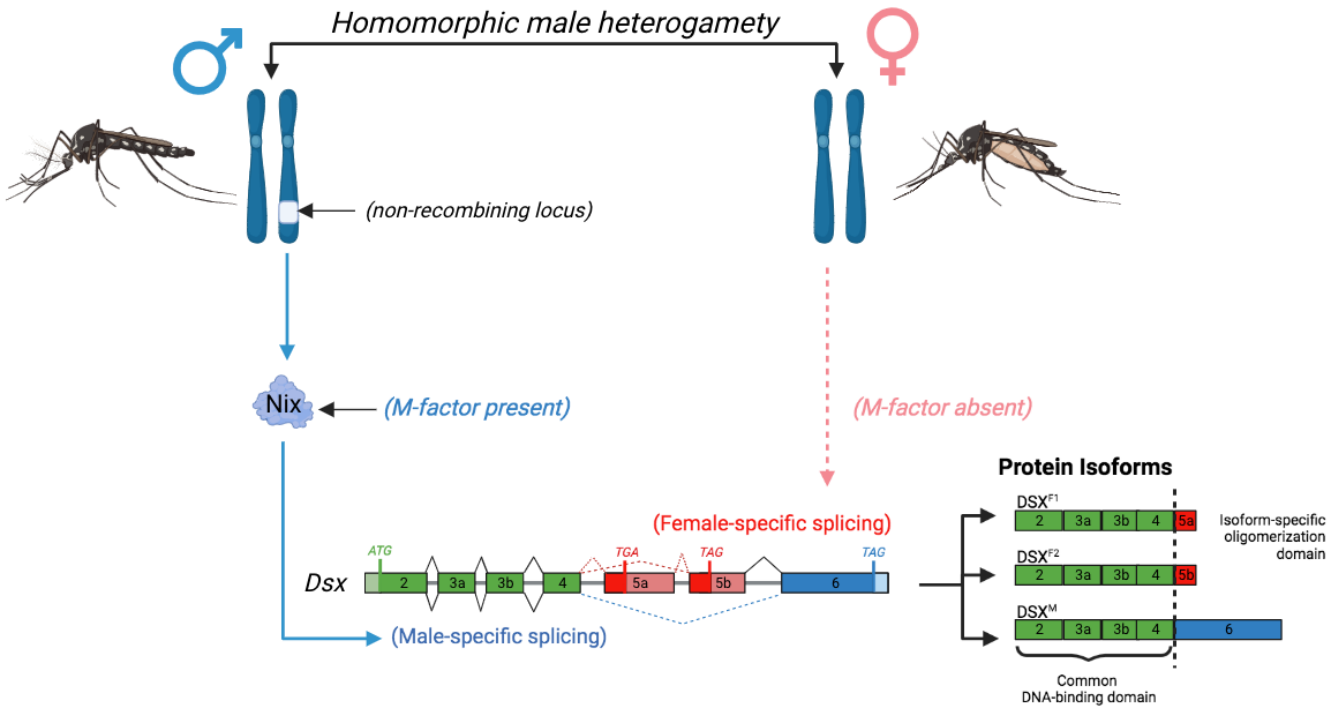

Figure 1. Sex-determination pathway in *Aedes aegypti*. Alternative splicing of *Doublesex* is mediated through the activity of Nix, the male-determining factor of *Aedes aegypti*. In the absence of *Nix*, female-splicing (red dashed lines) is the default, but two protein isoforms can result. In males, only one DSX isoform is predicted from the male-specific splicing (blue dashed lines). While all splice variants of *Doublesex* have identical DNA-binding domains, divergent protein interaction domains are believed to be responsible for differential gene expression patterns.

Figure 2. Protein sequence alignment comparing *Ae. aegypti* and *D. melanogaster* Doublesex. This figure separates the N-terminal, universal (top; common to both male and female isoforms) region from the female-specific (middle) and male-specific (bottom) C-

terminal regions. The non-sex-specific OD1 (containing the DNA-binding domain) is denoted and boxed with colours representing sequence similarities. The common and female-specific regions of the protein-interacting domain (OD2) are also denoted in coloured boxes, representing sequence similarities. Conservation scores immediately below the alignment denote identical peptides (*), highly similar amino acid substitution (+), or, for less similar amino acid substitutions a score of between 1 (low similarity) to 9 (higher similarity). Clustal Omega (EMBL-EBI) and Jalview software (University of Dundee) were used to perform and analyze the sequence alignments.

1.2.2 Differentially expressed transcripts

The basis for sexual dimorphisms is differential, sex-specific gene expression patterns (Ledón-Rettig et al., 2017). While the initial signal for this sexually dimorphic gene expression is derived from *Doublesex*, this transcription factor alone does not directly account for all differentially expressed transcripts (DETs) (Ledón-Rettig et al., 2017; Tomchaney et al., 2014). When studying sex-specific gene expression, researchers must account for differences in cell/tissue-type and timing of development. In one exemplary study, Tomchaney et al (2014) focussed on sexually dimorphic gene expression in the *Ae. aegypti* pupal brain. Based on the premise that sex-specific behaviours rely on differential development of the brain, the authors searched for differentially expressed transcripts in that tissue. By 24 hours post-pupation, there is significant restructuring of the adult brain, and thus, this timepoint was chosen for these studies. An initial cDNA microarray analysis comparing male and female transcript levels of 16,581 genes found 189 and 201 genes upregulated in male and female pupal brains, respectively (Tomchaney et al., 2014). These differentially expressed transcripts represented a variety of cellular processes including biosynthetic pathways, proteolysis, and cell growth and proliferation (Tomchaney et al., 2014). Through *in-situ* hybridization experiments combined with RNAi-mediated silencing, the authors further demonstrated the involvement of *doublesex* in the generation of DETs in the pupal brain (Tomchaney et al., 2014).

Microarray analysis also allowed Harker et al (2013) to observe differential, stage specific gene expression across six developmental phases in *Ae. aegypti*. Unsurprisingly, upon comparing the transcriptome of sex-sorted adults, the authors found differential expression between adult males and females (Harker et al., 2013). Significant DETs between adult males and females represented three main molecular functions: intracellular protein transport, vesicle-mediated transport, and DNA replication (Harker et al., 2013). The authors postulated that these genes are likely involved in sex-specific differences in immune function, as only females are vectors for flaviviruses such as dengue. While this study did not make tissue-specific comparisons between adult male and female mosquitoes, it illustrated the presence of distinct gene repertoires that exist between males and females, and differential gene expression across all stages of development.

While studies have demonstrated differential gene expression across sexes in pupae and adults, there remains to be a study examining sexually dimorphic gene expression in *Ae. aegypti* larval tissues. Researching sexually dimorphic gene expression in larvae would greatly assist with our understanding of sex-differentiation, but reliably sex sorting larvae is a difficult task due to a lack of visible sexual dimorphisms. As gene expression changes significantly throughout the developmental stages (embryonic, early-/late-larval, pupal, adult) of holometabolic insects, a complete understanding of sex-differentiation in mosquitoes would require sex-specific expression data from the larval stage. While difficult to find and clearly identify, the presence of a primordial gonopore on the 6th abdominal subsegment in 3rd instar males does allow for sex sorting, albeit at a painstakingly slow pace (Christophers, 1960). For faster throughput sex-sorting, transgenic *A. gambiae* mosquitoes, expressing a fluorescent protein under a male-specific (*e.g. Nix*) promoter have been developed (Magnusson et al., 2011). This system,

although not currently available, would be of great benefit in *Aedes aegypti*, allowing for earlier, more reliable sex-sorting of larvae.

1.2.3 Dimorphic anatomies, behaviours, and physiologies

The product of sex-differentiation is the manifestation of sex-specific characters. Males and females adopt unique behavioural, anatomical, and physiological features that are ultimately necessary for sexual reproduction. While adults are most easily distinguished based on sex, some sexually dimorphic features become apparent in larvae and pupae of some mosquito species (Christophers, 1960; Lehane, 2005; Lutrat et al., 2019). In culicine late-larvae, males and females exhibit size-dimorphisms, whereby males are generally smaller than females (Christophers, 1960; Lehane, 2005; Lutrat et al., 2019). The smaller males typically pupate and eclose before females, which allows for a narrow window of time available for sex-sorting to take place (Lutrat et al., 2019). How these dimorphisms in size and developmental timing arise is currently unknown. The larger size and slightly delayed development of female larvae could be the result of differential production of growth signals or differences in nutrient acquisition in the two sexes, but to date, no studies have explored the mechanisms underlying the subtle differences in the two sexes during the juvenile stages.

Anatomical features that can be used to discern males and females do additionally appear in late larval and pupal stages of *Ae. aegypti.* As noted above, microscopic inspections of late instar males can detect the primordial gonopore, for sex-sorting larvae (Christophers, 1960). Pupae can also be sexed by differences in the shape of the genital lobe at the terminal pupal subsegments (Christophers, 1960; Tomchaney et al., 2014). However, this process of sexing larvae and pupae on the basis of differential morphology is time-consuming and potentially more

damaging than size-sorting. Size-sorting, however, is usually only effective in separating the largest females from the smallest males; intermediate-sized individuals can be either sex.

Sexing adult *Ae. aegypti* is comparatively simple, as distinct morphological features can be seen with the unaided eye. Most easily identified are differences in antennal structure. Males have distinct, bushy 'plumose' antennae, contrasting the slender 'pilose' antennae of their female counterparts (Christophers, 1960). Differences in antennal structure and physiology allow for differential perception of odorants in the environment (Duman-Scheel and Syed, 2015). Females, guided by behaviours including blood feeding and oviposition use specialized antennae with specialized odorant receptors and three times the number of sensilla relative to males (Duman-Scheel and Syed, 2015).

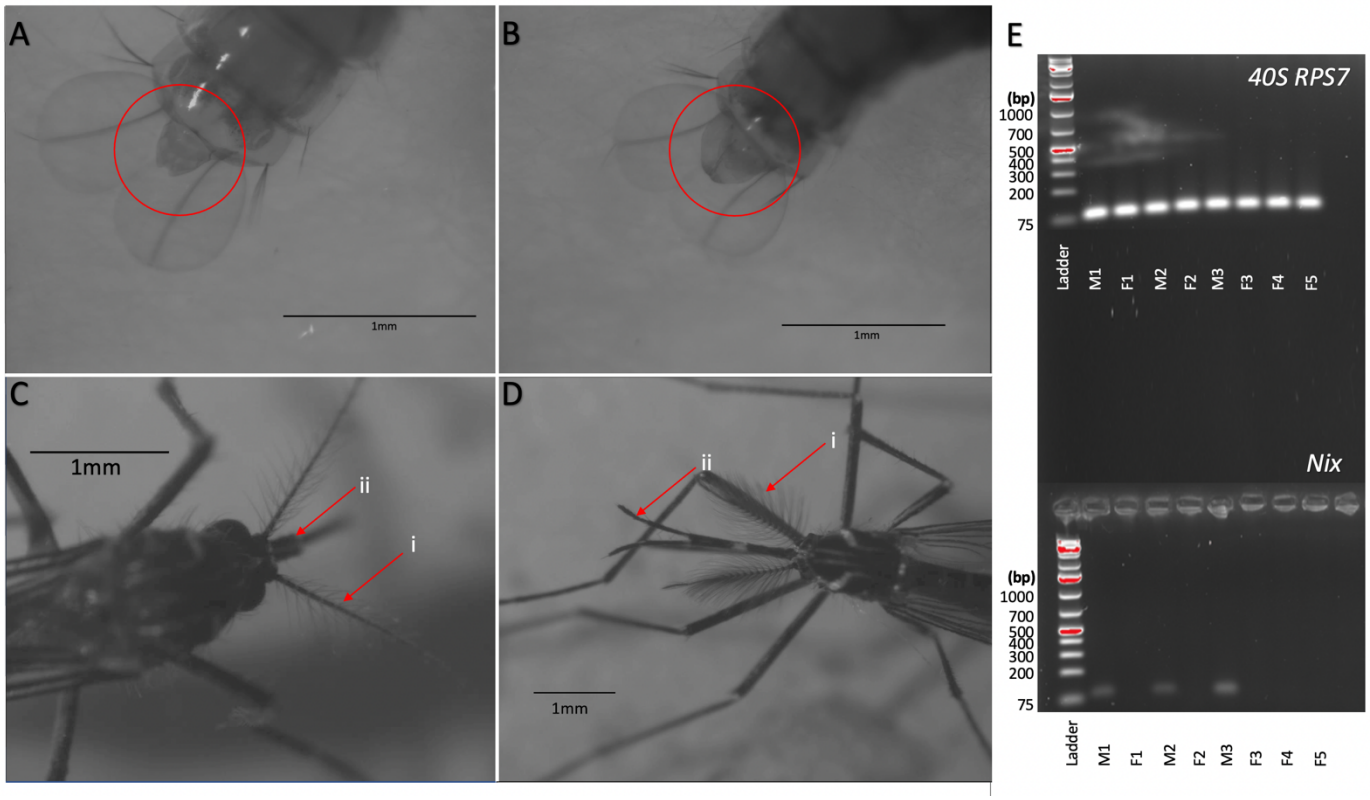

Figure 3. Sexual dimorphisms in *Aedes aegypti.* Structural dimorphisms are used to differentiate female pupae and adults (A & C, respectively) from male pupae and adults (B & D, respectively). Circles highlight sexually dimorphic terminal segments on pupae, arrows indicate sexually dimorphic features of (i) antennae and (ii) maxillary palps. Sex-limited expression of *Nix* (E), using RT-PCR analyses, can also be used to reliably sex sort mosquitoes at all life stages, including larvae, as illustrated in this PCR-based colony screen, where M1 – M3 are male (identified by the presence of 100 bp RT-PCR product), and F1 – F5 are female (absence of the Nix PCR product). Amplification of the 40S ribosomal protein S7 (top panel) in all samples confirmed that the RNA extractions and cDNA syntheses from each individual insect were successful.

Additionally, the sex-specific feeding behaviours of female mosquitoes necessitate unique structures and physiologies in their feeding structures and gastrointestinal system. While both sexes feed on nectar, females, with their need for extra protein to support egg development, require their characteristic slender, skin-piercing proboscis to obtain a bloodmeal (Christophers, 1960; Lehane, 2005). This behaviour also requires a unique internal anatomy and physiology

specialized for blood feeding and digestion (Lehane, 2005). These characteristics allow for the consumption of large bloodmeals (109% unfed body mass), rapid excretion of excess water, and proper digestion (Lehane, 2005).

Finally, male and female mosquitoes have distinct reproductive systems capable of tasks such as production of viable gametes and fertilization. Testes are found in males and used to produce sperm, whereas females have ovaries responsible for oogenesis (Lehane, 2005). Males have distinct structures including clasping terminalia and an aedeagus which, during mating, are responsible for grabbing onto females and delivering sperm into the genital chamber (Lehane, 2005). Aedine females generally only mate once and store the sperm in a specialized structure known as the spermatheca (Lehane, 2005). Stored sperm is then ultimately used to fertilize all eggs produced by a female in her lifetime (Lehane, 2005).

1.3 Applications in Insect Control

1.3.1 Selecting for male-only populations

Arboviruses such as dengue, zika, and yellow fever threaten millions of people globally, and currently the best method of control is population suppression of mosquito vectors (Whyard et al., 2015). Chemical insecticides are not only hazardous to the environment and human health, but pesticide-resistant strains of disease-vectoring mosquitoes are emerging, and thus, new methods of population control are desperately needed (Lutrat et al., 2019; Sanchez-Bayo et al., 2013; Whyard et al., 2015). In recent years, environmentally safer techniques dependent on the mass release of treated male mosquitoes have been considered. These methods include Sterile insect technique (SIT), *Wolbachia*-mediated cytoplasmic incompatibility, and Gene-Drive technologies (Li et al., 2019; Lutrat et al., 2019; Whyard et al., 2015; Zhang and Lui, 2020). The

release of only male mosquitoes is essential for each of these techniques as contaminating females can blood-feed, compete for resources, and distract released males (Lutrat et al., 2019; Whyard et al., 2015). The sterile insect technique involves the mass rearing, sterilization, and release of male mosquitoes which competitively mate with wild females (Whyard et al., 2015). As culicine females generally mate once in a lifetime, they will not have viable offspring. Cytoplasmic incompatibility is a phenomenon whereby mosquitoes infected with the intracellular pathogen, *Wolbachia* can only successfully mate with "compatible" partners (Zhang and Lui, 2020). In this case, a cross-between uninfected females and *Wolbachia*-positive males results in unsuccessful fertilization. Infected females can successfully mate with both infected and uninfected males, and *Wolbachia* is passed on to all subsequent progeny (Zhang and Lui, 2020). Thus, for the cytoplasmic incompatibility method to work, only *Wolbachia*-positive males must be released (Zhang and Lui, 2020). Finally, gene-drive technologies are a method of engineering a dominant lethal construct capable of achieving up to 100% inheritance (Li et al., 2019). For example, one may engineer a deleterious mutation impacting dsx^{F}. In this case, all subsequent progeny will develop as males, ultimately resulting in a population crash. Gene-drive technologies are inherently risky and rely on release of transgenic organisms, and hence are substantially more controversial (Li et al., 2019).

1.4 Research Objectives

Because of their relevance to human health and pronounced sexual dimorphisms, understanding sex development in mosquitoes can provide additional means of effective population control and improve our fundamental understandings of sex-determination and

differentiation. Although studies have improved our understanding of these processes in mosquitoes such as *Aedes aegypti,* many important questions remain.

1.3.1 OBJECTIVE 1: Compare expression levels and binding partners of DSX^{F1} and DSX^{F2}

In many higher Dipteran insects, such as *Drosophila sp., Musca sp.,* and even anopheline mosquitoes, *Doublesex* is spliced into only one male or one female specific isoform (Jin et al., 2021). In culicine mosquitoes however, two distinct female isoforms of *Doublesex* are produced (Price et al., 2015b). Characterizing the isoform-specific expression levels across development and identifying isoform-specific binding partners will provide insights into their relative importance across stages of development and may suggest reasons as to why multiple female isoforms are necessary.

1.3.2 OBJECTIVE 2: Identify DSX^{F}-interacting proteins essential for female development

Because both male- and female-specific isoforms of Doublesex have identical DNA-binding domains, it is believed that the sex-specific activity of Doublesex is the result of different protein-protein interactions occurring at isoform-specific oligomerization domains (Clough et al., 2014). Characterizing protein interactions of female Doublesex isoforms may identify new genes that may be targeted to impact female-development. The role of these genes in female development will be assessed through dsRNA-mediated transcript knockdown experiments with a focus on impacts to female-specific mortality, sex ratios, and developmental timing.

2 MATERIALS AND METHODS

2.1 Rearing of Insects

Aedes aegypti adults were reared at 25°C, 50% humidity with a photoperiod of 16:8h (light:dark). Mosquitoes were provided a 10% sucrose solution as nourishment and provided fresh rat blood weekly to enable egg development in females. *Aedes aegypti* eggs were collected on a moist paper towel and allowed to develop for a minimum of one week. Eggs were hatched in deoxygenated water. Hatched larvae were then placed in a large plastic container containing tap water and rabbit-feed pellets at 28°C until they reached the pupal phase of development, when they were then transferred to $1m^3$ screened breeding cages.

2.2 Isolation of RNA and cDNA Synthesis

RNA was purified from the whole body of *A. aegypti* individual or pooled mosquitoes. Between 1 to 5 insects were placed in 300µL Lysis Buffer (GeneJET RNA purification kit; Thermofisher) supplemented with 2% β-mercaptoethanol. Tissues were then homogenized using a Bullet Blender® (Next Advance), and total RNA was purified using the GeneJET RNA purification kit (Thermo Fisher Scientific). Purified RNA samples were stored at -80°C. cDNA synthesis was performed using a qScript cDNA Supermix kit (Quanta Biosciences). Purity of cDNA and absence of genomic contamination was assessed using PCR amplification using Lucigen EconoTaq PLUS 2X Master Mix (according to manufacturer's protocol) using *40s ribosomal protein (s7)*-specific primers in *A. aegypti* (Table A1). Agarose gel electrophoresis was then performed using ethidium bromide to visualize the samples.

2.3 Sex-sorting of Aedes aegypti

Other than a translucent, primordial gonopore seen in male 4th instar, *Aedes aegypti* larvae have no distinct morphological characteristics amenable to sex-sorting based on appearance, and thus, a genetic screen was developed for individual larvae. Contrary to all other RNA isolation and cDNA synthesis reactions, for the purposes of sex-sorting, individual 2nd and 3rd instar larvae, and the Cells-to-cDNA™ II Kit (Thermofisher) was used. Homogenization of individual larvae was performed using a mortar (PCR tube) and pestle (flamed pipette tip) in 25µL of ice-cold lysis buffer. Upon homogenization, an additional 75µL volume of lysis buffer was added, and the lysis reaction was allowed to proceed at 75°C for 10 minutes. cDNA was synthesized from the lysate, according to the manufacturer's protocol, and a PCR screen was used to assess for the presence of the male-specific gene, *Nix*. Using Lucigen EconoTaq PLUS 2X Master Mix with primers specific for *Nix* (male-specific gene), and *rpS7* (positive control) (Table A1), the sex of each individual larva was determined (Figure 3 E).

A similar sex-sorting genetic screen was performed for 4th instar larvae, however, due to the large amount of tissue, the GeneJet RNA Purification Kit (Thermofisher) with Bullet Blender® (Next Advance) homogenization was used for RNA extractions. TURBO™ DNase (Invitrogen) was used to remove genomic DNA contamination and cDNA was synthesized using qScript cDNA Supermix (Quanta Biosciences). Genetic screens were performed as described above to determine the sex of each larva. Following verification, pools of cDNA were pooled based on stage and sex for downstream applications. Extracted RNA samples and synthesized cDNA samples were stored at -80°C and -20°C, respectively.

In pupae, sex can be reliably determined based on tail morphology (Figure 3, A & B), allowing for non-lethal sex-sorting. Morphological features were also used to sex-sort adult

mosquitoes (Figure 3 C & D). Individual insects were pooled into groups of 5, based on sex and stage and RNA extractions, DNase treatments, and cDNA synthesis were performed using GeneJet RNA purification kits, TURBO™ DNase, and qScript cDNA Supermix, as described previously.

2.4 Quantitative Reverse Transcriptase PCR (qRT-PCR) Analysis

qRT-PCR was used to assess relative levels of isoform-specific *Doublesex* gene expression in *A. aegypti* across stages of development. As an internal control, a fragment of the *A. aegypti s7* gene was amplified to normalize the amount of cDNA added to the qRT-PCR reactions. qRT-PCR was performed in the BioRad CFX Connect Real-Time PCR System using SsoFast Evagreen Supermix (BioRad) according to manufacturer's specifications. To ensure specificity and consistency of PCR products, melting curve analyses were performed. Technical duplicates of each reaction were performed to ensure precision, and quantification of transcript levels was assessed according to the $2^{-\Delta\Delta CT}$ value method (Livak and Schmittgen 2001).

2.5 Expression of His-tagged Doublesex Proteins and GST-tagged Binding Partners

cDNA derived from sex-sorted *Ae. aegypti* pupae was used as template for PCR amplification of each isoform of *Doublesex,* and two binding partners (GST-677 and GST-810) identified in the ensuing protein pulldown and mass-spectrometry analysis. Primers designed to amplify the entire coding sequence of each isoform also included restriction sites on their 5' end to facilitate restriction-ligation into their respective plasmid (Table A1).

The plasmid pBAD/*Myc*-His A (Invitrogen) was selected for the bacterial expression of Doublesex isoforms whereas pGEX-6P-1 (Sigma) was used for expression of the pulldown partner proteins. To amplify the coding sequence of each Doublesex isoform, forward and reverse primers contained 5' NcoI and HindIII restriction sites, respectively, and products from these reactions were gel-extracted and digested using respective FastDigest (Thermofisher) restriction enzymes. The pBAD/Myc-His plasmid was similarly digested with NcoI and HindIII restriction enzymes. The full-length coding sequence of the pulldown partner Ribosomal Protein Subunit RPB8 (GST-677) was amplified using forward and reverse primers containing 5' XhoI restriction sites, and a truncated version (for ease of cloning and higher predicted stability) of mRNA cap guanine N-7 methyltransferase (GST-810) was amplified with forward and reverse primers both containing 5' EcoRI restriction sites. Identical restriction sites were used for forward and reverse primers due to limited compatibilities. Thus, for digestion of the amplified CDS of GST-677 only XhoI was used, whereas for GST-810 only EcoRI was used. The plasmid pGEX-6P-1 was similarly digested with respect to the GST-677 and GST-810 digests.

Digested products were subject to agarose gel electrophoresis followed by extraction using the E.Z.N.A.® Gel Extraction Kit (Omega). Ligation of the purified digestion products into similarly digested plasmids was performed using T4 DNA Ligase (Invitrogen). Ligation products were then transformed into competent *E. coli* DH5a cells (Thermo Scientific) and grown overnight at 37^{o}C on Luria-Bertani (LB) + [50 μg/mL] ampicillin plates. To confirm the successful transformation, the E.Z.N.A.® Plasmid DNA Mini Kit (Omega) was used to extract and purify plasmids which were subjected to PCR screening and sent for Sanger sequencing (Peter Gilgan Centre for Research and Learning, Toronto, Ontario). Upon confirmation of successful transformation, purified plasmids were transformed into the protease-deficient *E. coli*

BL21 (Thermo Scientific). Resulting colonies were subject to PCR-based colony screening and subsequently grown up for small-scale protein expression trials.

100 μL of overnight cultures of transformed BL21 were used to inoculate 10 mL of LB broth with [100 μg/mL] ampicillin. These 10 mL cultures were grown to an OD_{600} of 0.6 and 100μL of 20% filter-sterilized Arabinose was added to induce protein expression of Doublesex proteins, whereas a final concentration of 1 mM IPTG was used to induce expression of GST-677 and GST-810. Cells were grown with shaking overnight at 20°C, pelleted, and washed with ice-cold Tris-buffered saline (25mM Tris, pH 7.2; 0.15M NaCl). Ice-cold Pierce™ Pull Down Lysis Buffer (Thermo Scientific) supplemented with Halt™ Protease and Phosphatase inhibitor (Thermo Scientific) facilitated cell lysis. Western blotting was employed to detect expression of the His-tagged fusion protein, using 6x His monoclonal antibodies (Invitrogen), Goat Anti-mouse IgG HRP conjugate (Sigma Aldrich), and Immobilon Forte Western HRP Substrate (Millipore). Detection of GST-tagged proteins was facilitated through protein isolation using Pierce™ Glutathione Magnetic Agarose Beads (Thermofisher) according to manufacturer's specification, followed by SDS-PAGE and Coomassie staining.

2.6 Large Scale Induction and Purification of Fusion Proteins

After confirming the successful bacterial expression of the female Doublesex isoforms (DSX^{F1}, DSX^{F2}), and the GST-tagged DSX binding partners, large-scale expression of the fusion proteins was conducted. A starter culture of 50 mL LB + [100μg/mL] ampicillin was inoculated and grown overnight, shaking at 37°C. 15mL of the starter culture was then added to 1.5L of LB + [100mg/mL] ampicillin and grown at 37°C until reaching an OD_{600} of 0.6. To induce expression of His-tagged DSX proteins, filter-sterilized L-Arabinose was then added to a final

concentration of 1% (w/v). For expression of GST-tagged pulldown targets, filter-sterilized IPTG was added to a final concentration of 1mM. Induced cells were then grown for 16 hours, shaking at 20°C.

Cell pellets were then obtained through centrifugation for 30 minutes at 4,100xg, 4°C (TX-1000 rotor, Thermofisher™). Upon removal of media, cells were resuspended in 50mL of filter-sterilized wash buffer (50mM Tris, 500mM NaCl, 20mM Imidazole) and (50 mM Tris pH 7.5, 200mM NaCl, 2mM β-mercaptoethanol) for His-tagged and GST-tagged proteins, respectively. To accommodate the predicted pIs (ProtParam Tool, Expasy) of each His-tagged fusion protein (DSX^{F1} = 8.09, DSX^{F2} = 7.29), the pH of the wash buffers used were adjusted to pH = 8.80 and pH = 8.02, for DSX^{F1} and DSX^{F2}, ensuring optimal binding to the nickel column. Cells were stored at -80°C prior to lysis and protein purification.

High-pressure homogenization of cells was performed using the Emulsiflex-C3 (Avestin). Prior to cell lysis, a final concentration of 1mM of phenylmethylsulfonyl fluoride (PMSF), 10mM of $MgCl_2$, and pinhead-sized amount of lyophilized DNase (approximately 0.1mg/mL) was added to the cells suspended in buffer. Homogenization was conducted according to the manufacturer's protocol at a pressure of 15,000 PSI. The cell lysate was then collected on ice and subsequently centrifuged for 30 minutes at 17,000xg, 4°C to separate the soluble lysate (containing the expressed protein) from the insoluble material.

2.7 Purification of His-tagged proteins

To capture the 6xHis tagged Doublesex proteins, the cellular lysate was then subjected to gravity-fed affinity chromatography column purification using 8mL of Nickel NTA agarose resin (GoldBio). The resin, stored in 20% ethanol, was washed with molecular grade water, charged

with one column volume (1 CV; approximately 40mL) of 200mM $NiSO_4$, washed again with 1CV of molecular grade water, and equilibrated into the wash lysis/wash buffer used for the respective protein (50 mM Tris pH 8.02 – 8.8, 500mM NaCl, 20 mM imidazole). Once equilibrated with wash buffer, the lysate was run through the column and washed with 200mL of wash buffer. This was followed by protein elution using 50mL of elution buffer (50mM Tris pH 8.02 or 8.8, 500mM NaCl, 500mM imidazole). The column was then discharged using 200mM EDTA pH 8.0, and washed with 1 CV of water, and stored in 20% ethanol. At each step (pellet, lysate, flow-through, wash, and elution) 15uL of sample was collected and run on an SDS-PAGE gel (Figure 7).

2.8 Purification of GST-tagged proteins

GST-810 and GST-677 were purified using a gravity-fed affinity chromatography column with 8mL glutathione-sepharose resin (Cytiva). To preserve the glutathione-sepharose resin, an initial cleaning of the lysate was performed by running the sample over a Q-sepharose column (10mL of resin in a 50mL gravity column). The Q-sepharose column was first washed with water, followed by an equilibration with lysis buffer (50 mM Tris pH 7.5, 200mM NaCl, 2mM β-mercaptoethanol). Following column equilibration, the lysate was run over the column and flow-through collected. Regeneration buffer 1 (50 mM Tris pH 8.8, 1M NaCl) was then used to wash the column, followed by a wash with water and storage in 20% ethanol.
The glutathione-sepharose column was washed with water and equilibrated in wash buffer (50 mM Tris pH 7.5, 500 mM NaCl, 2 mM β-Mercaptoethanol). The flow through from the Q-sepharose column was then run over the column, followed by 200 mL of wash buffer. The protein of interest was then eluted using 50 mL of elution buffer (50 mM Tris pH 7.5, 500 mM

NaCl, 20 mM glutathione; glutathione was added immediately prior to use and pH was adjusted to 7.5). The glutathione-sepharose resin was then washed with 50 mL each of regeneration buffer 1, regeneration buffer 2 (20 mM sodium acetate pH 4.5, 1M NaCl), water, and then equilibrated and stored in 20% ethanol. The eluted GST-tagged protein was then subject to overnight dialysis (4^{o}C in lysis buffer) followed by concentration using a centrifugal filter with a 10kDa cut off (Amicron).

2.9 Size Exclusion Chromatography

For use in protein pull-downs followed by mass-spectrometry, eluted 6-His tagged Doublesex proteins were subjected to fast performance liquid chromatography (FPLC) with complete buffer exchange using the ÄKTA pure (GE Healthcare) and a HiLoad 16/600 superdex 75 gel filtration column (GE Healthcare). Before use, the column (stored in 20% ethanol), was washed with 240 mL of molecular grade water, followed by 240 mL of filtered gel filtration buffer (20 mM Tris-HCl pH 8.00 – 8.80, 100 mM NaCl, 1 mM β-mercaptoethanol). Prior to addition of protein to the ÄKTA, proteins were concentrated to a volume of approximately 2 mL using a centrifugal filter (Amicron) with a 10 kDa molecular weight cut-off. Fractions containing the purified Doublesex proteins were verified using SDS-PAGE, collected, concentrated again, flash frozen in liquid nitrogen, and stored at -80^{o}C.

2.10 Aedes aegypti nuclear extractions

The nuclei of *Aedes aegypti* pupae were extracted using the NE-PER™ nuclear and cytoplasmic reagents (Thermofisher), according to manufacturer specifications. Briefly, 100 mg of sex-sorted mosquito pupae were collected and gently homogenized in ice-cold buffer using a

mortar and pestle. An initial membrane disruption using cytoplasmic extraction reagents, followed by centrifugation (4ºC, 16,000xg) allowed for removal of cytoplasmic proteins, while leaving nuclei intact. Nuclear extraction reagent was then added to extract out nuclear proteins which was followed by an additional centrifugation step (4ºC, 16,000xg) to remove insoluble debris of the nuclear envelope. The collected nuclear fractions were flash frozen and stored at -80ºC.

2.11 Nuclear Protein Pulldowns and Mass Spectrometry

HisPur™ Ni-NTA Magnetic Beads (Thermofisher) were used to bind 0.300 mg previously purified, fusion Doublesex proteins according to the manufacturer's protocols. Bound proteins underwent a series of 3 washes in wash/equilibration buffer (25 mM Tris-HCl, 0.15 M NaCl, pH 7.2). After the final wash, 400 µL of nuclear lysate was added to the beads and allowed to incubate in an end-over-end rotator at 4ºC overnight. After 16 hours of incubation, a series of 5 additional 400 µL washes were used to remove any unbound proteins and any trace amounts of detergent. Beads were then resuspended in 50 µL of wash/equilibration buffer and transported to the Manitoba Centre for Proteomics and Systems Biology for mass spectrometry. Controls included the bead-bound fusion proteins without nuclear extract, and nuclear extract incubated with beads.

2.12 Confirmation of Mass Spectrometry Analysis using GST-Pulldowns

To confirm protein-binding interactions discovered in the mass-spectrometry analysis, the previously purified GST-tagged fusion proteins, GST-677 and GST-810, were used to facilitate pulldowns of previously purified His-tagged Doublesex using Pierce™ Glutathione Magnetic

Agarose Beads (Thermofisher). Briefly, 100 μg of either 6His-DSX^{F1} or 6His-DSX^{F2} was incubated with 100μg of either GST-677 or GST-810 in a total volume of 400μL wash buffer (125 mM Tris pH 7.4, 150 mM NaCl, 1 mM DTT, 1 mM EDTA). Protein mixtures were then added to previously equilibrated glutathione magnetic beads, vortexed briefly, and mixed at room temperature on an end-over-end rotator for 90 minutes. Following incubation, beads were collected against a magnetic stand and the supernatant discarded. Beads were then washed four times with 400 μL volumes of wash buffer, mixed gently, and supernatant discarded. Elution of proteins was facilitated by the addition of 250 μL of elution buffer (125 mM Tris pH 7.4, 150 mM NaCl, 1 mM DTT, 1 mM EDTA, 50mM glutathione; glutathione added immediately before elution and pH readjusted to 7.4) followed by a 10-minute incubation on the end-over-end rotator. The elution step was repeated twice, with beads collected against a magnetic stand and supernatant (containing proteins of interest) collected. Eluted proteins were then subject to Western-Blotting as described earlier, using mouse Anti-His monoclonal antibodies to detect the His-tagged DSX proteins.

2.13 Bacterial dsRNA Expression

To determine the impact of transcript knockdown of putative DSX-interacting proteins identified in the mass-spectrometry analyses, RNA interference (RNAi) was employed using a bacterial expression system to produce dsRNA. Briefly, each dsRNA was designed to 350-450 bp of the target mRNA transcript. Constructs were PCR-amplified using primers listed in Table A1 and blunt-end ligated into pJET 1.2 using T4 DNA ligase (Thermofisher). Following transformation into competent *E. coli* DH5a cells, individual colonies containing the correct plasmid inserts were grown overnight in a broth culture and subsequently used for plasmid

purification using the E.Z.N.A.® Plasmid DNA Mini Kit (Omega). Now flanked by XbaI and XhoI restriction sites, the dsRNA templates were digested out of pJET 1.2 and ligated into a similarly digested pL4440 using T4 DNA ligase. The resulting pL4440 including the dsRNA template was then transformed into competent *E. coli* DH5a, and, following plasmid isolation using the E.Z.N.A.® Plasmid DNA Mini Kit (Omega), the plasmid was transformed into the destination vector, *E. coli* HT115, a tetracycline resistant, nuclease deficient strain.

Previously performed experiments determined the optimal parameters for dsRNA induction trials (Giesbrecht, unpublished data). To induce expression of dsRNA for use in knockdown assays, overnight cultures of transformed *E. coli* were grown in LB with ampicillin [100 μg/mL] and tetracycline [12.5 μg/mL] shaking overnight (225 rpm, 37^{o}C) and subsequently used to inoculate 200 mL of LB + ampicillin + tetracycline, in a 500 mL baffled flask. Cultures were grown under the same conditions until reaching an optical density of 0.6, and IPTG was then added to a final concentration of 0.6 mM. Following induction with IPTG, cells were grown for an additional 4 hours and subsequently collected through centrifugation at 3,750xg for 10 minutes.

Pelleted cells were then resuspended in 3mL of 100mg/mL brewer's yeast slurry, and 12 mL of molten 1% agar. The resulting resuspended cell mixture was then incubated in an 80^{o}C hot water bath for 10 minutes to heat kill all bacteria. The heat-killed bacterial mixture was then allowed to cool until the agar was near solidification to avoid settling of the brewer's yeast. This cooled mixture was then vortexed once more to ensure total homogeneity and immediately transferred to clean, open-topped 10 mL syringes and stored at 4^{o}C.

2.14 Bacterial Feeding of dsRNA to Mosquito Larvae

RNAi-mediated transcript knockdown of genes identified from mass-spectrometry analysis was performed using the bacterial-agar plugs described previously. Briefly, *Ae. aegypti* larvae were hatched in deoxygenated water and placed in groups of 20 into deep dish petri plates with approximately 100-150 mL of dH_2O. Larvae were provided 0.5 mL bacterial plugs over the duration of the experiment (containing dsRNA) to consume *ad libitum* and as their sole source of nutrition. Developmental timing from larva to pupa, and pupa to adult were recorded in the context of the respective sex. Mortality and sex ratios were also recorded, as were any physical anomalies of the resulting adults.

2.15 Sex-biased protein expression analysis

When sending nuclear pulldown samples for mass spectrometry analysis, The Manitoba Centre for Proteomics and Systems Biology kindly offered to perform mass spectrometry analysis comparing proteomes of pools of 10 male and 10 female pupae, sex sorted based on tail morphology (Figure 3). After conducting 1D mass spectrometry analysis, quantities of each protein were approximated as the sum of MS/MS intensities for all peptides derived from the isolated proteins. These data were searched for sex-biased genes by comparing approximate protein abundances, using an arbitrary threshold of ≥ 1 and ≤ -1 difference of the Log_2-scaled data (i.e. $\geq$2-fold difference in protein abundance between the two sexes of pupae).

3 RESULTS

3.1 Isoform specific expression of Dsx transcripts across larval and pupal development

qRT-PCR analyses were used to examine the accumulation of DSX^{F1} and DSX^{F2} isoform transcripts across the different stages of mosquito development. Both DSX^{F1} and DSX^{F2} show a progressive increase in expression with developmental age, and higher expression of DSX^{F2} compared to DSX^{F1}. The data from these assays demonstrated significantly higher mRNA accumulations of DSX^{F2} compared to DSX^{F1} in pupae (362%) and adults (398%) ($p<0.0001$) (Figure 4), while no significant differences in the levels of the two isoforms were identified in larvae.

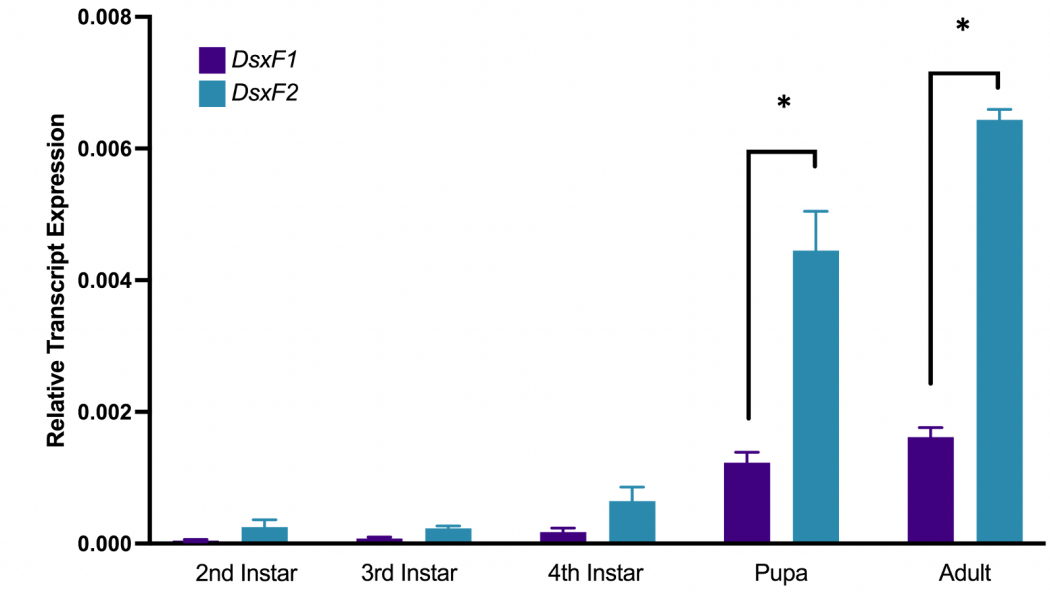

Figure 4. Expression of *Dsx^{F1}* and *Dsx^{F2}* during mosquito development. cDNA obtained from pools of female larvae and individual pupae and adults were subjected to qRT-PCR analysis using primers from Table A1, with *Ribosomal protein subunit 7 (Rps7)* as a reference gene. Statistically-significant differences in expression between *Dsx^{F1}* and *Dsx^{F2}* were observed in pupae ($p<0.0001$) and adults ($p<0.0001$), ANOVA with Šídák post-hoc (denoted by the asterisks).

3.2 Expression of Recombinant DSX Proteins

PCR amplification of DSX coding sequences confirmed that DSX^{M}, DSX^{F1}, and DSX^{F2} expression was strictly limited to the respective sex (Figure 5). Following the successful ligation into pBAD-*Myc*-His A, a western blot of His-DSX^{F1} and His-DSX^{F2} small-scale induction trials detected expression of the expected fusion proteins following the addition of L-Arabinose to a final concentration of 2% (Figure 6).

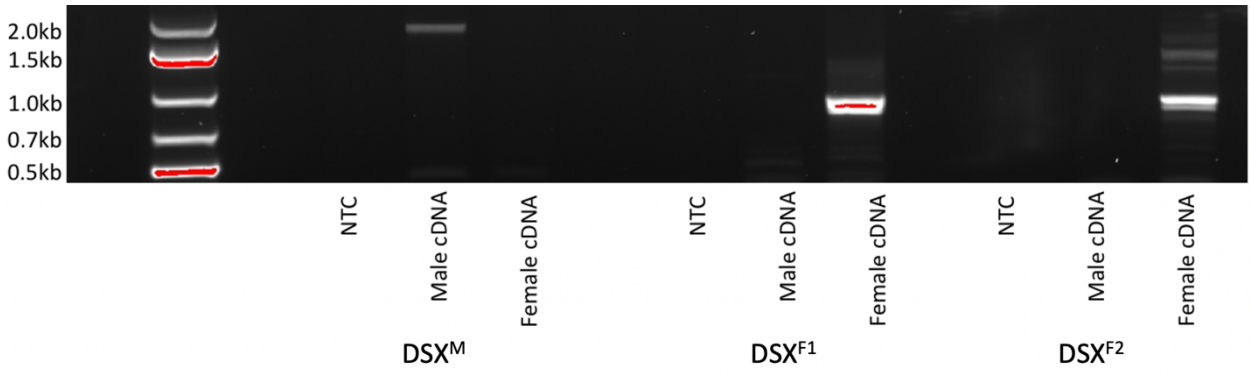

Figure 5. Sex-limited expression of *Doublesex* isoforms in *Aedes aegypti*. Full-length CDS of male- (1,669 bp) and female-specific isoforms (F1 788 bp; F2 815 bp) were successfully PCR-amplified from cDNA pools of the cognate sex. NTC = non-template control, to ensure no genomic DNA was present. Sanger sequencing was used to confirm the identity of the inserts following insertion into destination vector. Faint bands observed above the predominant DSX^{F2} represent non-specific amplification products resulting from lower stringency PCR conditions. Gel extraction was used to isolate the predominant PCR products, avoiding contamination of non-specific products.

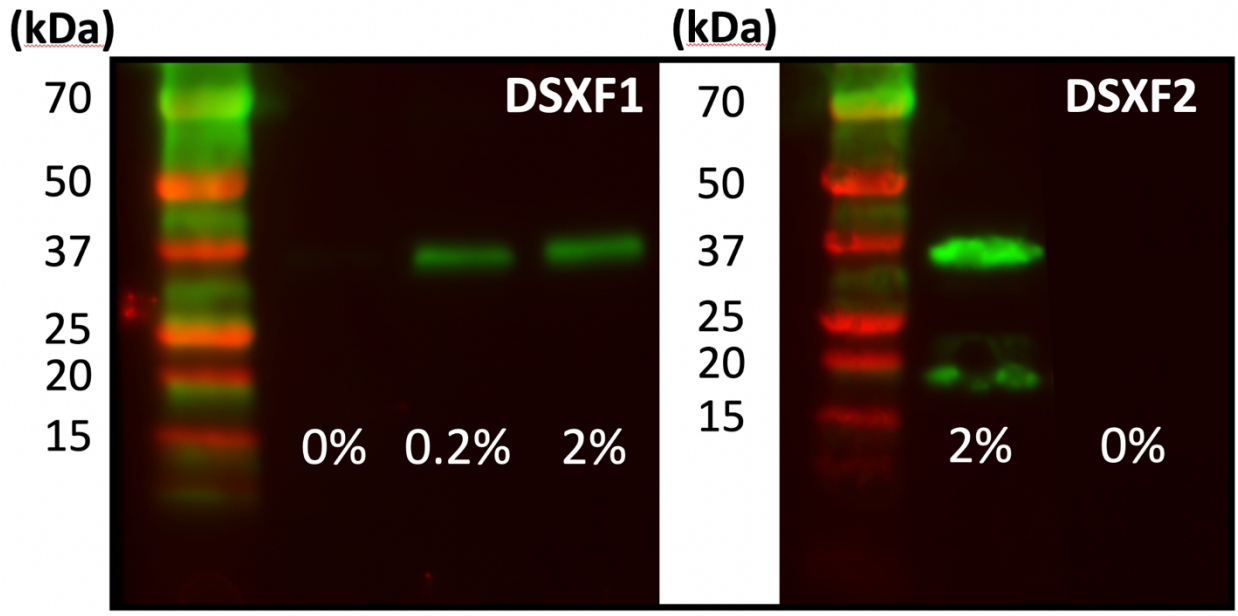

Figure 6. Small scale bacterial expression of 6xHis-tagged DSX^{F1} and DSX^{F2} proteins, of the expected ~33 kDa mass, visualized using western blot with chemiluminescence detection. Percentages denote the final concentrations of L-Arabinose used to induce protein expression, with only 2% being used for DSX^{F2} and both isoforms in all subsequent experiments. The lower (~17 kDa) molecular weight band observed in DSX^{F2} is likely a degradation product containing the N-terminal His-tag.

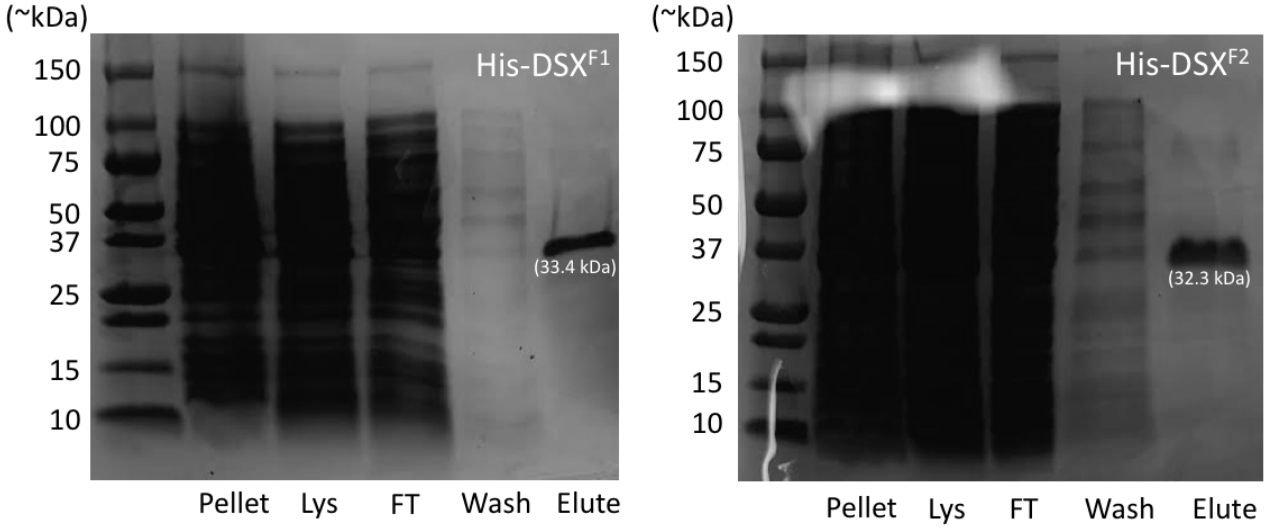

Figure 7. Detection of His-tagged Doublesex following nickel column purification. 15uL of pellet, lysate, flow through, wash, and elution fractions from nickel column purification were all sampled and resolved using SDS PAGE with True Blue Safe Stain. Expected band sizes were found in the eluted fraction for His-DSX^{F1} (33.4 kDa) and His-DSX^{F2} (32.3kDa).

Large-scale expression and FPLC-purification of His-DSX^{F1} and His-DSX^{F2} following a gel filtration chromatography (Superdex 75) yielded 1.87mg and 2.00mg of purified, concentrated proteins, respectively (Figure 8). A double-peak was observed on the gel filtration elution chromatograph, and is suspected to be the *E. coli* protein, DnaK in the sample, as this chaperone protein is frequently found to bind fusion proteins in bacterial expression systems and has a similar hydrodynamic radius of the dimerized DSX proteins. SDS-PAGE was used to confirm the presence and identity (based on size) of His-DSX^{F1} (33.4 kDa) and His-DSX^{F2} (32.3 kDa).

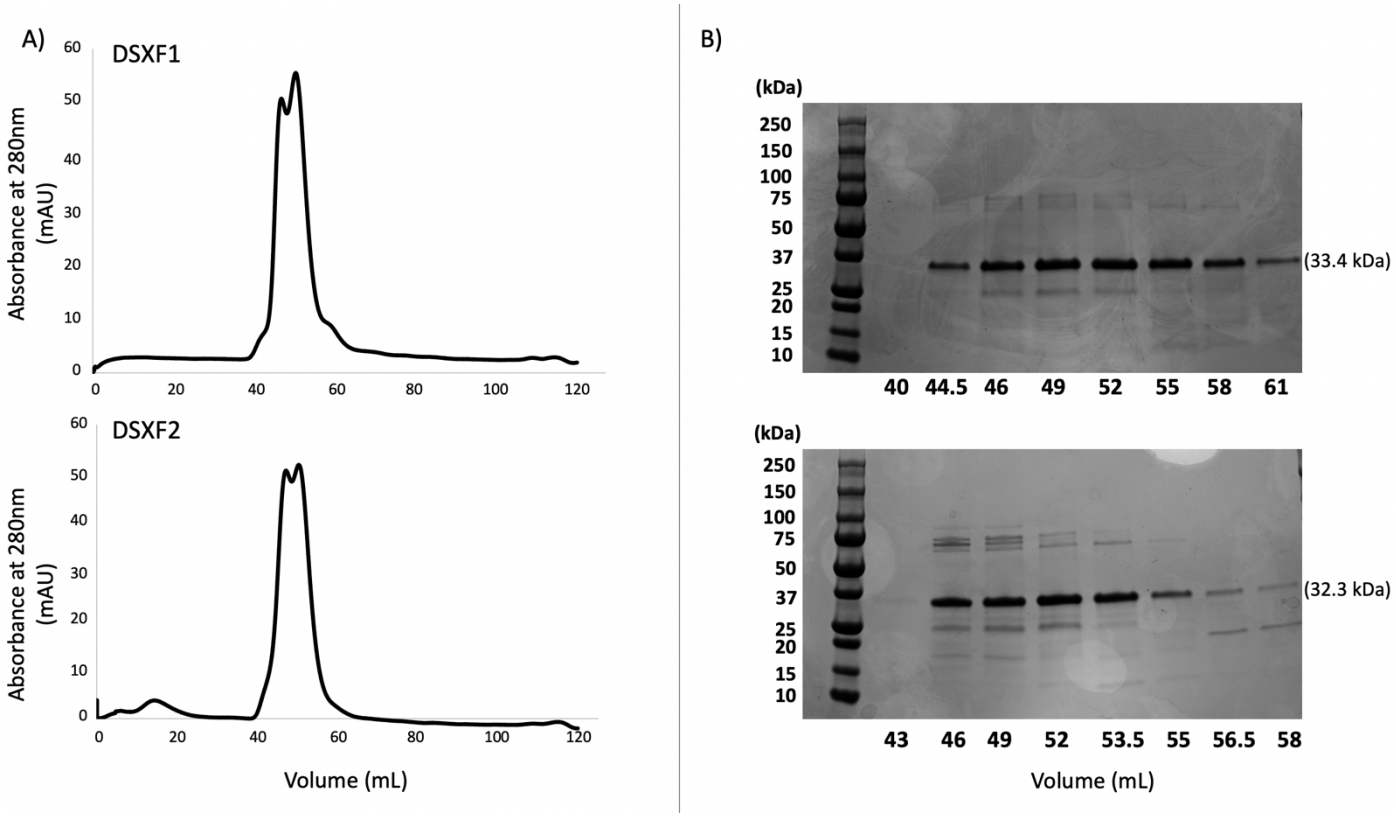

Figure 8. FPLC purification of 6xHis-tagged DSX^{F1} and DSX^{F2} proteins. A) A280 was used to determine the eluted fractions of purified fusion proteins, collected in fractions 44 to 61. B) Proteins within those fractions were subsequently verified using SDS-PAGE with Coomassie staining. The expected 33.4kDa and 32.3 kDa DSX^{F1} and DSX^{F2}, respectively, are the predominant proteins isolated.

3.3 Prospective DSX^{F} Binding Partners Determined in Mass Spectrometry Analysis

From two rounds of mass-spectrometry analyses, a total of 50 unique proteins were identified as being more highly enriched in the bead fractions containing the Doublesex Bait proteins, compared to nuclear lysate alone (Table A2). In the assays conducted in this study, the identified proteins were at least 2-times more abundant in the DSX-containing samples than the negative control samples. From the 50 identified proteins, 12 were selected for subsequent RNAi-mediated knockdown analysis, based on characteristics such as high affinity for DSX^{F1} or DSX^{F2}, nuclear localization, and/or nucleic acid binding or transcriptional regulatory activity (Table 1). Two of these proteins, AAEL000677 and AAEL021810, were additionally studied in further pulldown experiments to confirm the binding interactions. Furthermore, of the 50 binding partners identified, seven demonstrated enrichment exclusive to the DSX^{F1} and 11 demonstrated a greater than 2-fold affinity uniquely for DSX^{F2}. Of the 12 gene targets selected for subsequent RNAi-mediated knockdown, 9 demonstrated similar moderate or high levels of affinity for both isoforms, whereas one (AAEL010847) demonstrated a unique affinity for DSX^{F1} and two demonstrated a unique affinity for DSX^{F2} (AAEL010514 and AAEL021400).

Table 1. Selection criteria for 12 gene targets identified in mass spectrometry analysis

Gene Target	Accession	Selection Criteria
DNA-directed RNA polymerase subunit rpb8	AAEL000677, XM_001649743.1	Nuclear localization; involvement in transcription
WD repeat-containing protein 48 homolog	AAEL021400 XM_021840350.1	Nuclear localization; ubiquitination activity
Glutamate synthase	AAEL014768, XM_021841419.1	High binding affinity
SEC63	AAEL025151, XM_021857125.1	High binding affinity
Aspartyl-tRNA synthetase	AAEL011655, XM_001661774.1	Nucleic acid binding activity
Aminoacyl-tRNA synthetase auxiliary protein	AAEL010514, XM_001650634.1	Nucleic acid binding activity
Succinyl-CoA ligase beta subunit	AAEL011746, XM_001661816.1	High binding affinity
Nop14	AAEL014051, XM_001657290.2	Nuclear localization, RNA binding
mRNA cap guanine-N7 methyltransferase	AAEL021810, XM_021856968.1	Nuclear localization, nucleic acid binding activity, gene regulation
PWI domain-containing protein	AAEL023022, XM_021838104.1	Nuclear localization, RNA binding activity
Zinc finger protein	AAEL010847, XM_001661028.1	Nuclear localization, nucleic acid binding activity
CAF1C_H4-bd domain-containing protein	AAEL027479, XM_001660533.2	Nuclear localization, high binding affinity

3.4 Expression of Recombinant Proteins for DSX Pulldown Assays

To confirm binding interactions observed in mass spectrometry analysis, two proteins were selected for further expression and pulldown experiments with DSX^F. The Ribosomal

protein subunit RPS8 (AAEL000677) and mRNA cap guanine-N7 methyltransferase (AAEL021810) were selected based on binding affinity, nuclear localization, predicted stability, and moderate size. While the full-length CDS of AAEL000677 was expressed, a truncated version of AAEL021810 was used due to improved predicted stability, based on a ProtParam Instability Index (Expasy) score of 37.99. Generally, an instability index lower than 40 predicts a more stable protein. Large scale expression and purification of two GST-tagged proteins identified as potential DSXF binding partners yielded 8.9 mg and 13.9 mg of concentrated GST-067 and GST-810, respectively (Figure 9).

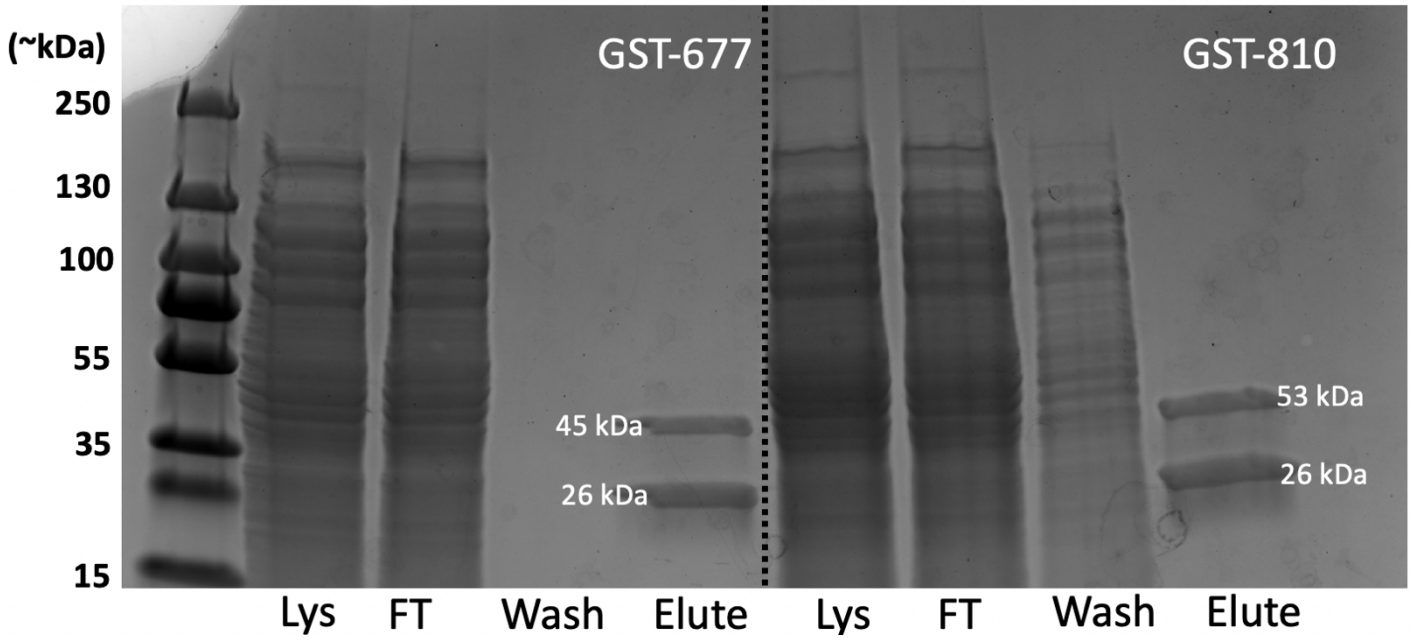

Figure 9. Large scale purification of GST-tagged DSX^{F} binding partners (AAEL000677 and AAEL021810). 15uL of lysate, flow through, wash, and elution fractions from glutathione sepharose column purification were all sampled and run on SDS PAGE with True Blue Safe Stain. Expected band sizes were found in the eluted fraction for GST-677 (45 kDa) and GST-810 (53kDa) with an additional band at 26 kDa expected to be Glutathione S-transferase.

3.5 Confirmation of DSX^{F1} and DSXF^{2} Binding Interactions through Protein Pulldowns

Pulldowns of His-DSX^{F1} and His-DSX^{F2} facilitated by GST-677 and GST-810 bound to glutathione magnetic beads were used to confirm two protein binding interactions observed in the mass-spectrometry analysis, where both DSX^{F1} and DSX^{F2} were observed to interact with the proteins encoded by the AAEL000677 and AAEL021810 genes. Following elution from beads, western blots were used to detect the His-tagged Doublesex proteins co-eluted with the prospective binding partners. These were compared to positive controls (concentrated His-DSX^{F1} and His-DSX^{F2}), and negative controls (eluted GST-proteins without His-DSX^{F1}/HisDSX^{F2}, His-DSX^{F1}/His-DSX^{F2} incubated on beads without GST-proteins, and concentrated GST-proteins). In the glutathione bead pulldowns, neither DSX^{F1} nor DSX^{F2} were detected in the absence of GST-tagged proteins AAEL000677 and AAEL021810. However, when the GST-tagged proteins were mixed with either DSX^{F1} (33.4 kDa) or DSX^{F2} (32.3 kDa), the appropriate sized bands were observed. The presence of DSX^{F1} and DSX^{F2} bands from GST-pulldowns (and not in His-DSX^{F} incubated on beads) supports the previous binding interactions observed of both AAEL000677 and AAEL021810 to both DSX^{F1} and DSX^{F2} (Figure 10).

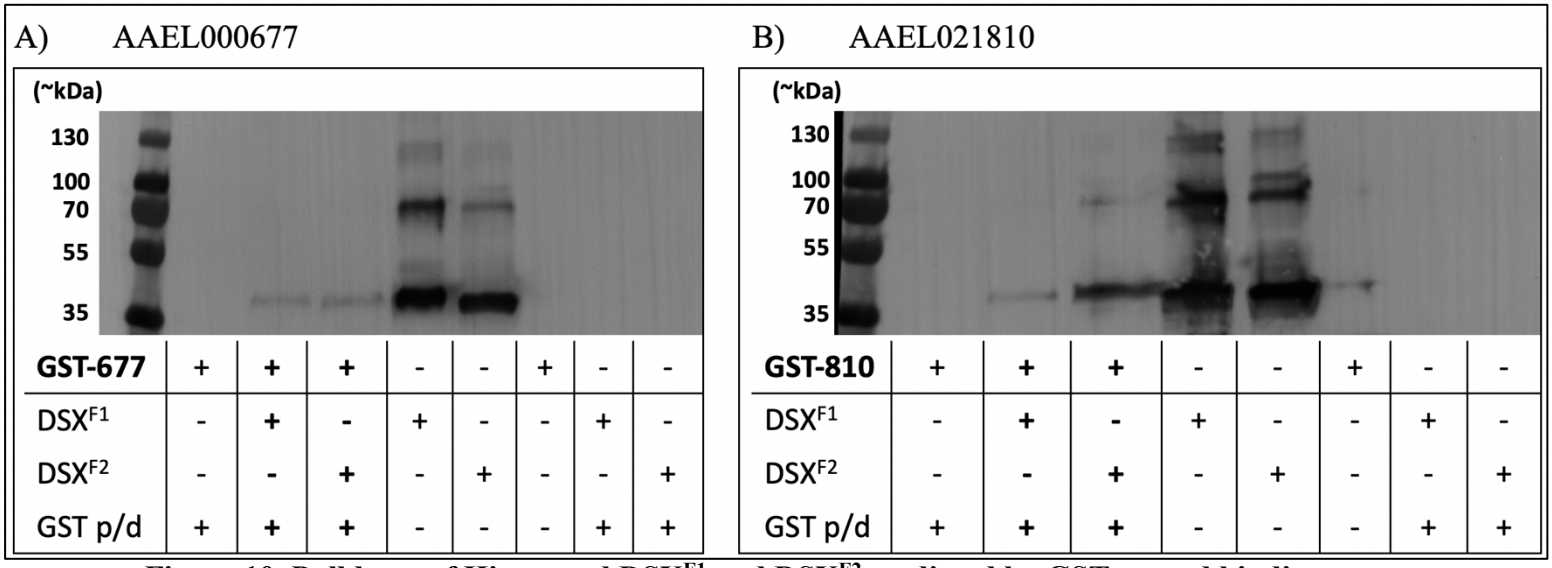

Figure 10. Pulldown of His-tagged DSX^{F1} and DSX^{F2} mediated by GST-tagged binding partners, (A) GST-677 and (B) GST-810, on glutathione agarose beads. Pulled down His-tagged Dsx^{F1} (33.4 kDa) and DSX^{F2} (32.3 kDa) were visualized using western blotting with anti-His monoclonal antibodies and colorimetric detection (alkaline phosphatase, BCIP). Presence (+) or absence (-) of GST-tagged proteins (GST-677 or GST-810) and His-tagged proteins (DSX^{F1} or DSX^{F2}) is indicated below each lane, as well as whether (+) or not (-) glutathione pulldown (GST p/d) was performed. In the case of GST p/d (-), concentrated proteins were added as reference.

3.6 Impacts on mosquito development following consumption of bacterial dsRNA

In total, 12 different dsRNAs, targeting genes identified in the mass spectrometry assay, were bacterially-expressed and fed to larvae to determine their impacts on mosquito development compared to pellets generated from bacteria containing an "empty" plasmid (a plasmid lacking a dsRNA construct) negative control. Briefly, parameters of interest included timing of pupation and eclosion relative to negative control treatments, delay between male and female pupation and eclosion, sex ratios, and survival.

Summarized in Table 2, of the 12 dsRNA constructs tested, 6 of these demonstrated significant differences in the time interval between male and female development. Female mosquito larvae fed on negative control bacteria eclose, on average, 1.1 days later than males,

but four dsRNAs caused the female larvae to accelerate their development, reducing the time gap in eclosion of the two sexes, while two dsRNAs caused statistically significant increases in the female larval development (Figure 11). Additionally, 5 of the 12 dsRNAs demonstrated significantly higher mortality, and 3 of the 12 were found to significantly skew sex ratios in favour of males (Table 2). Based on their significant, female-specific impacts to mortality and/or developmental timing, 5 of these 12 dsRNAs were considered of special interest with their data illustrated in Figure 12. Interestingly, two proteins demonstrating exclusive affinity for DSX^{F2} (21400 and 10514) resulted in significant impacts to development, whereas 10847 (demonstrating exclusive affinity for DSX^{F1}) did not.

Table 2. Summary of dsRNA feeding assay data

dsRNA Name	Gene Target	Accession	Altered Sex Ratio	Mortality	Emergence Gap
00677	*DNA-directed RNA polymerase subunit rpb8*	AAEL000677, XM_001649743.1	M > F p<0.01	21.3% p<0.05	n.s.
21400	*WD repeat-containing protein 48 homolog*	AAEL021400 XM_021840350.1	M > F p<0.05	n.s.	Increased p<0.0001
14768	*Glutamate synthase*	AAEL014768, XM_021841419.1	M > F p<0.05	31.7% p<0.0001	Decreased p<0.0001
25151	*SEC63*	AAEL025151, XM_021857125.1	n.s.	45.0% p<0.0001	n.s.
11655	*Aspartyl-tRNA synthetase*	AAEL011655, XM_001661774.1	n.s.	23.3% p<0.05	Increased p<0.05
10514	*Aminoacyl-tRNA synthetase auxiliary protein*	AAEL010514, XM_001650634.1	n.s.	26.7% p<0.01	Decreased p<0.0001
11746	*Succinyl-CoA ligase beta subunit*	AAEL011746, XM_001661816.1	n.s.	n.s.	Decreased p<0.0001
14051	*Nop14*	AAEL014051, XM_001657290.2	n.s.	n.s.	Decreased p<0.05
21810	*mRNA cap guanine-N7 methyltransferase*	AAEL021810, XM_021856968.1	n.s.	n.s.	n.s.
23022	*PWI domain-containing protein*	AAEL023022, XM_021838104.1	n.s.	n.s.	n.s.
10847	*Zinc finger protein*	AAEL010847, XM_001661028.1	n.s.	n.s.	n.s.
27479	*CAF1C_H4-bd domain-containing protein*	AAEL027479, XM_001660533.2	n.s.	n.s.	n.s.

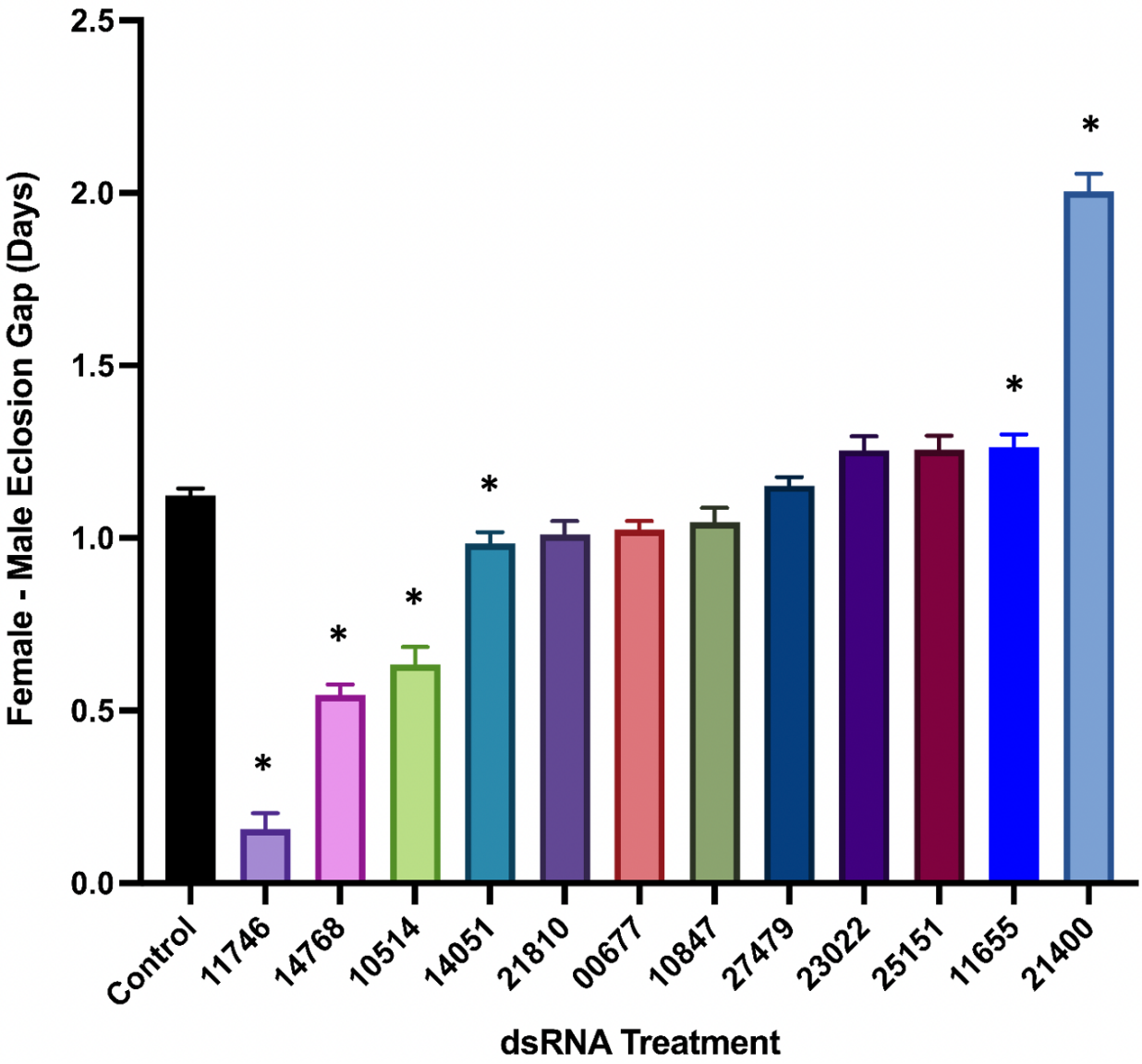

Figure 11. Interval between male and female eclosion is impacted by the consumption of various dsRNAs targeting genes identified in mass spectrometry. Values refer to means and standard errors of the absolute difference between male and female developmental timing from hatch to eclosion. Statistical significance between negative control and treatments was determined using one-way ANOVA with Dunnett's multiple comparisons test.

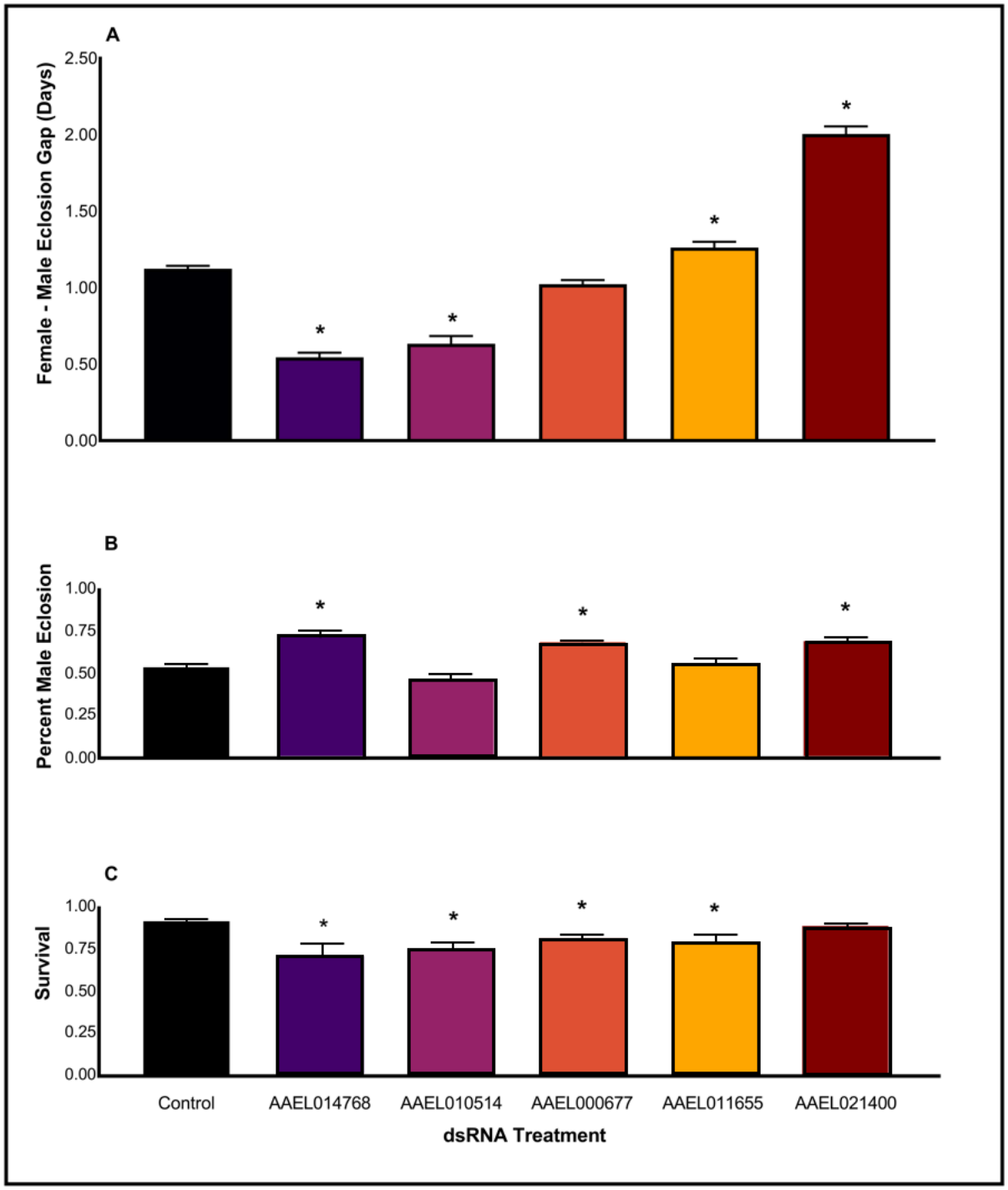

Figure 12. Altered female development following consumption of dsRNA targeting transcripts from mass-spectrometry analysis. The 5 dsRNA treatments demonstrating the most significant impacts to female development are illustrated using data from Table 2. Parameters assessed included male/female developmental gap (A), male-female sex-ratios (B), and mortality (C). Statistically significant differences relative to negative control were determined using one-way ANOVA with Dunnett's multiple comparison test (A) or binomial tests (B & C).

3.7 Impact of temperature on dsRNA treatments

After conducting bacterial feeding treatments at 28ºC, it was hypothesized that a lower temperature (and consequently slower development) could increase the emergence gap between male and female mosquitoes. The same treatments were repeated at 22ºC with dsRNA previously demonstrated to accelerate (AAEL021810) and delay (AAEL021400) female development relative to males. In all treatments, a decrease in temperature demonstrated a significant increase in the interval between male and female pupation relative to the respective 28ºC treatment. The dsRNA targeting AAEL021400 demonstrated the greatest difference, a 142% ($p<0.0001$) further delay in female pupation, relative to males, between the 22ºC and 28ºC treatments (Figure 13). Of note, by lowering the temperature, it is possible to collect a higher percentage of the male pupae, without contaminating females (Figure 14), when the larvae were fed the dsRNA targeting AAEL021400. At 28ºC, males, free of any contaminating females, could only be collected on day 6, and only 5.7% of the males could be salvaged at this early time point. In contrast, when the temperature was lowered to 22ºC, 63% of the males could be collected by day 11, without any contaminating females. For sex-sorting applications, this delayed female development could prove useful.

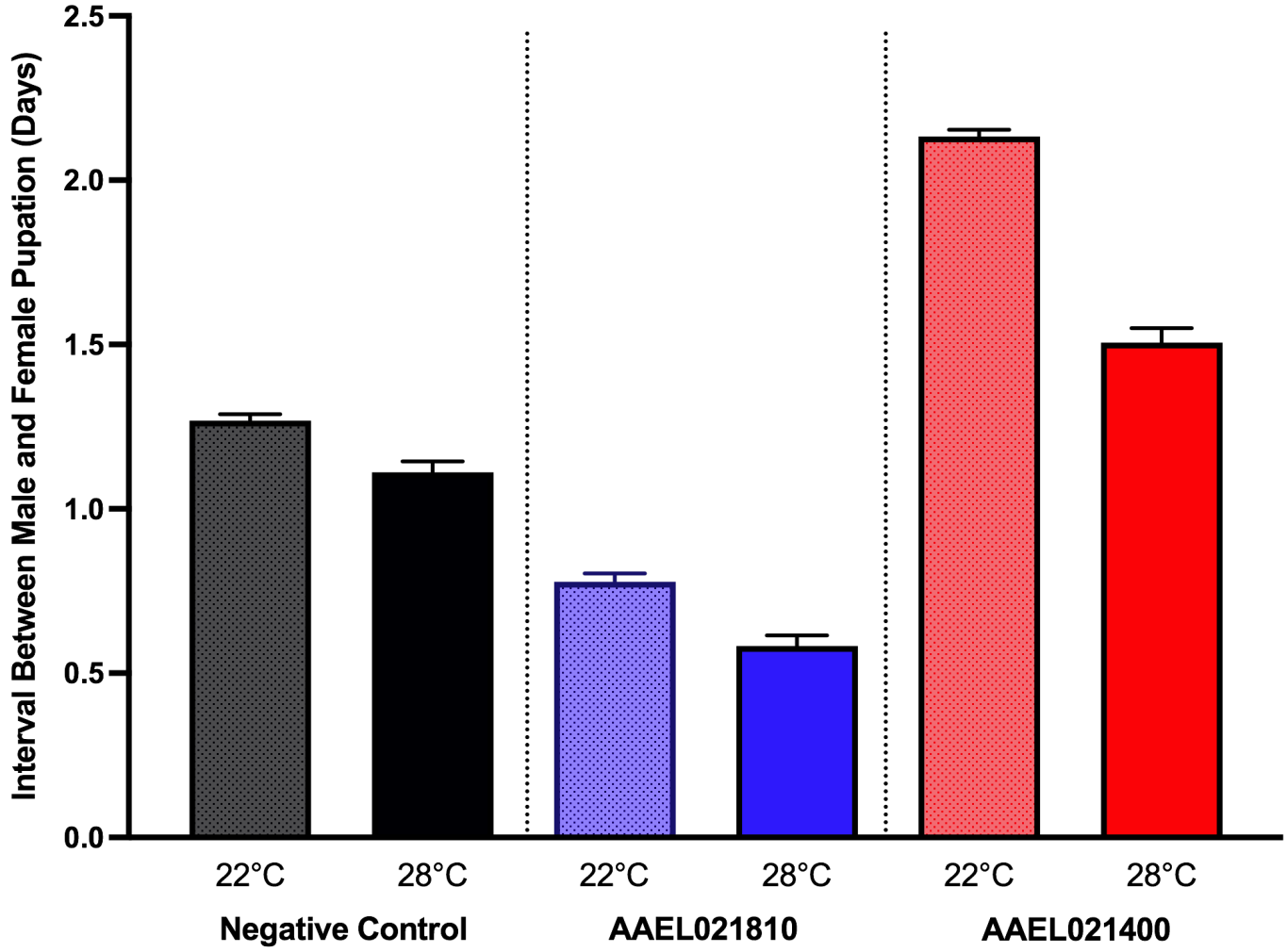

Figure 13. Impact of temperature on dsRNA treatments and male-female pupation interval. DsRNAs demonstrating accelerated (AAEL021810) and delayed (AAEL021400) female development were tested at both room temperature (~22ºC) and 28ºC. Statistically significant differences ($p<0.001$) were observed across all treatments (1-way ANOVA with Tukey's test for multiple comparisons).

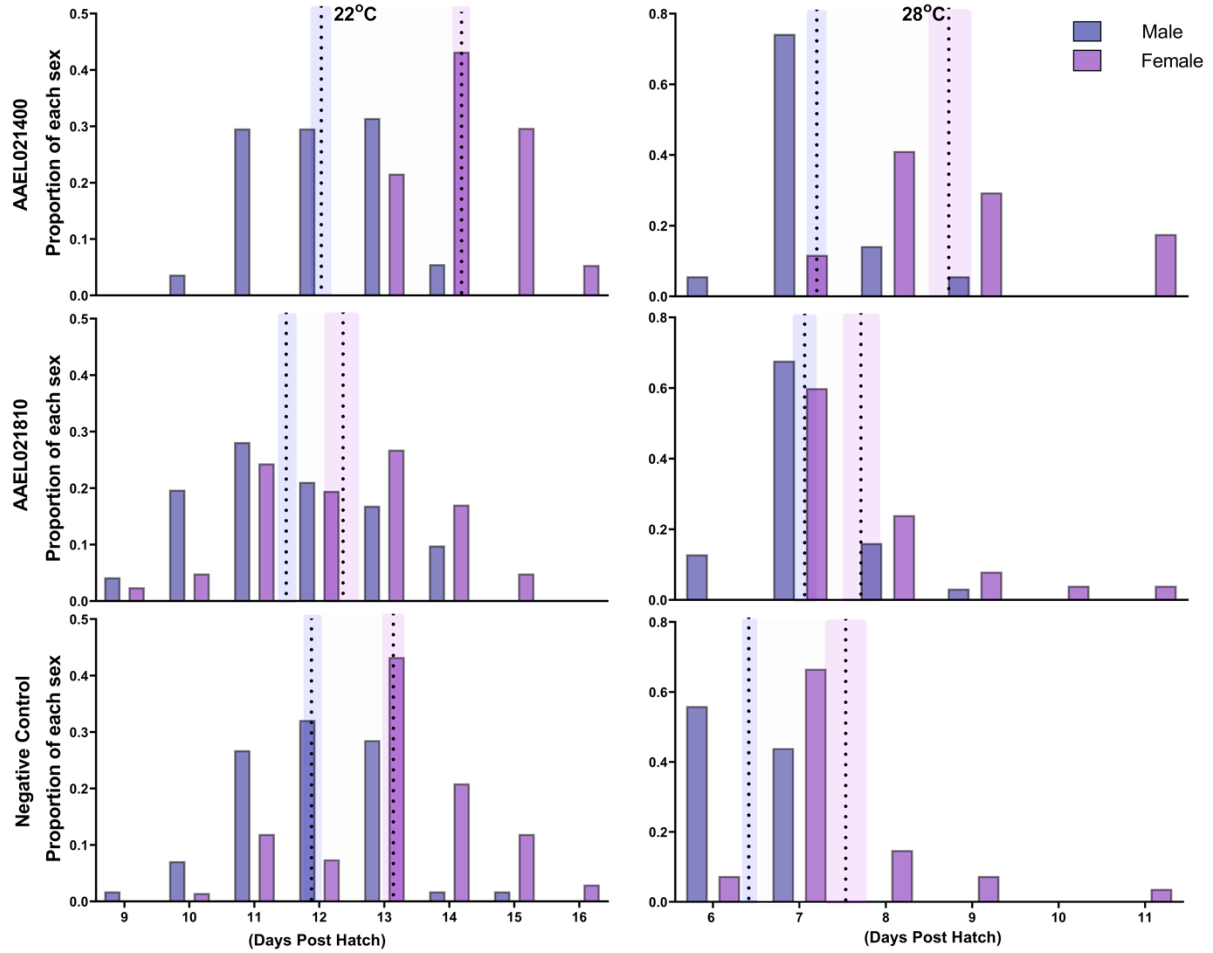

Figure 14. Impact of temperature and dsRNA treatments on pupation timing. Proportion of males and females pupating on each day post hatch and are illustrated by solid blue (male) and magenta (female) columns. Dotted lines indicate average day of pupation with ± SEM indicated by the width of the surrounding faded blue (male) or magenta (female) columns.

3.8 Sex-biased protein expression

Proteomic analyses of male and female pupae identified 735 and 405 proteins that had greater than 2-fold abundance relative to the opposite sex in female and male pupae, respectively. Of these proteins, 447 were exclusively detected in females and 286 in males. While these proteins demonstrating exclusively male or female expression are notable, Figure 15 illustrates those genes which show sex-bias (greater than 2-fold expression, but not exclusive) of

which, 288 and 119 are female- and male-biased, respectively. The full list of proteins are included in a supplemental electronic file 1. Of note, the DSX proteins were not found in this proteomic screen, which suggests that some proteins may have been missed.

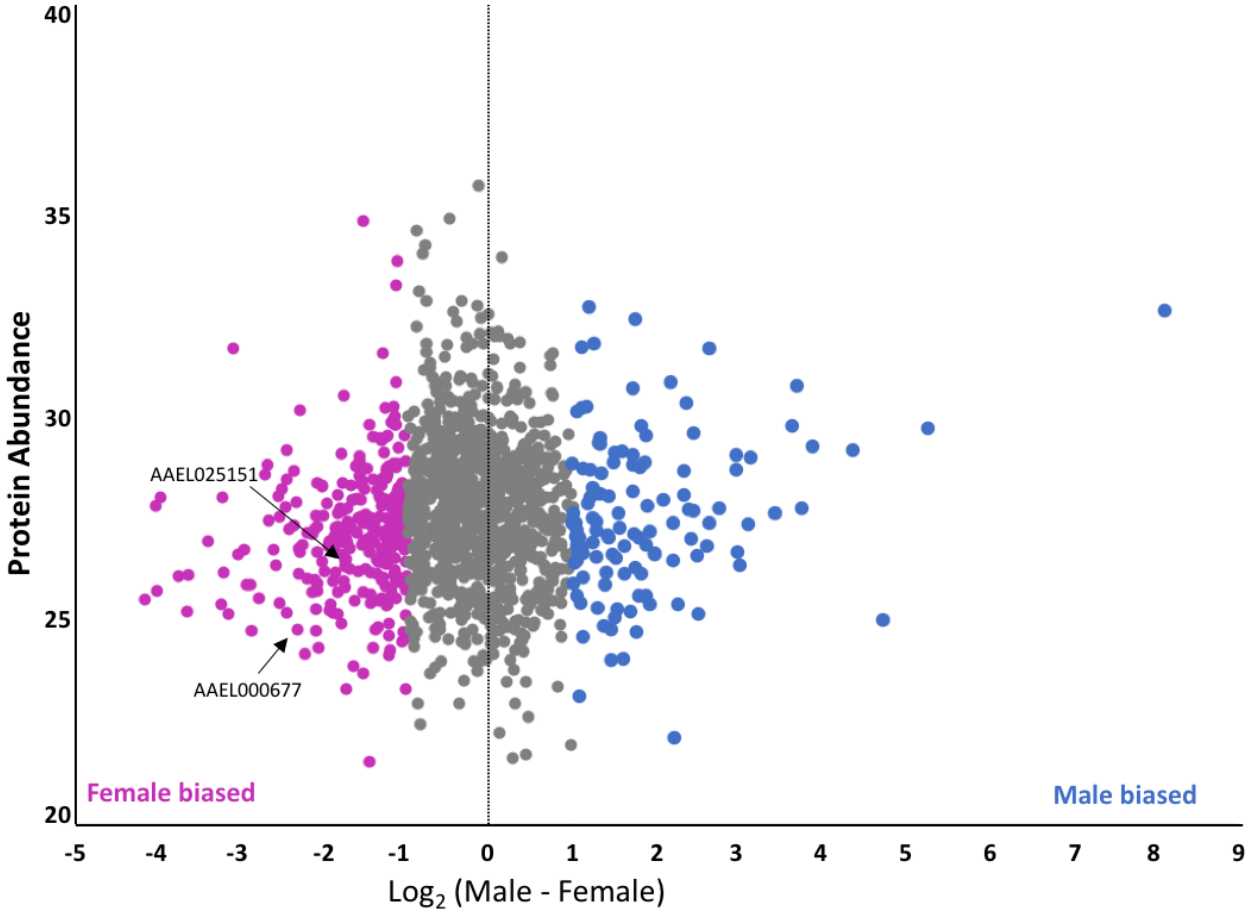

Figure 15. Sex-biased protein expression. Approximate abundances of each protein were calculated as the sum of (MS/MS) and Log_2 transformed. Pink and blue dots represent female and male biased (but not exclusive) proteins, respectively. Grey dots represent proteins with less than the arbitrary 2-fold difference in protein abundance between males and females. Two genes from the dsRNA feeding assays, AAEL0252151 and AAEL000677, were observed as female-biased and are highlighted in the figure.

4 DISCUSSION

At the end of the sex-determination pathway, Doublesex isoforms function to guide sex-specific gene expression patterns, ultimately leading to the sexually dimorphic features seen in mosquitoes. Particularly, when all DSX isoforms bind identical DNA consensus sequences, it is the isoform-specific binding partners that are believed to facilitate the divergent responses to gene expression patterns. This study focussed on the two female-specific DSX isoforms, DSX^{F1} and DSX^{F2}, to determine several binding partners that are essential for female development. A comparison with the binding partners of the male isoform, DSX^{M}, will be part of a future study.

4.1 Comparisons between DSX^{F1} and DSX^{F2}

In many dipteran insects such as *Drosophila melanogaster, Bactrocera dorsalis*, *Musca domestica*, and anopheline mosquitoes, *Dsx* pre-mRNA is spliced into either one male or one female isoform (Jin et al., 2021). In Culicidae, however, multiple female-specific isoforms have been observed (Price et al., 2015b). Additional insect phyla such as Lepidoptera (butterflies and moths), and Coleoptera (beetles) have also been observed to have multiple female-specific isoforms, which may contribute to the rapid evolution of *Doublesex* (Cho et al., 2007; Deshmukh et al., 2020). While both female isoforms were expressed across development, this study's findings demonstrated consistently higher expression of DSX^{F2} compared to DSX^{F1}, despite DSX^{F1} having the highest similarity to DSX^{F} in *D. melanogaster* (Figure 2). Notably, of the target proteins tested in the knockdown experiments, knockdown of binding partners exclusive to DSX^{F2} demonstrated significant developmental impacts, whereas knockdown of the binding partner exclusive to DSX^{F1} did not. It is possible that DSX^{F2} represents the major female-specific isoform, guiding most essential roles in female development. Observations in *Papilio sp.*

(swallowtail butterflies), similarly identified one female-specific isoform as the major isoform across stages of development (Deshmukh et al., 2020). While my study demonstrated a high level of DSX^{F2} expression compared to DSX^{F1} across development, it did not examine whether the two female isoforms differed in their tissue-specific expression. Having two similar, yet distinct female isoforms could provide an extra degree of tissue-specific control for sexually dimorphic gene expression patterns. Future studies could consider tissue-specific expression of the different isoforms during the various development stages of the insects, and additionally explore the different splicing factors responsible for the distinct isoforms.

From the mass-spectrometry analysis, DSX^{F1} and DSX^{F2} demonstrated significant overlap in binding partners, with a few isoform-specific exceptions (Table A3). This could be explained by the similar functions, yet the possibility of tissue- or cell type-specific control required for the DSX^{F} isoforms. Rice et al. (2019), demonstrated the need for spatiotemporal control of DSX activity in *D. melanogaster*, since not all tissues demonstrate sexual dimorphisms to an equal degree. While *Drosophila* do not have multiple female isoforms to achieve this gradient of differential gene expression patterns, in *Ae. aegypti,* the dimerization activity of DSX along with two distinct isoforms presents three possible $DSX^{F1/F2}$ complexes, each of which may have different affinities for other transcription factors. Tissue and stage-specific expression differences were observed across the three female *dsx* isoforms in *Papilio* swallowtails, indicating an extra level of regulation for sex-differentiation (Deshmukh et al., 2020). While RNAi of Dsx^{F} demonstrated female-specific lethality when fed to larvae (Whyard et al., 2015), pupal microinjections of siRNAs targeting a sequence common across all *dsx* isoforms did allow analysis of a knockdown phenotype in adult *Ae. aegypti* (Mysore et al.,

2015). Pupal microinjections of dsRNAs targeting either *dsx*^{F1} or *dsx*^{F2} could additionally be used to compare possible tissue-specific impacts following knockdown.

4.2 Identification of new targets for female-specific development

The dsRNA feeding experiments provide evidence that the female DSX isoforms bind to proteins that play a role in female development. Relative to the negative control, feeding dsRNA specific to 8 of the 12 genes identified in the mass-spectrometry assay resulted in statistically significant differences observed for at least one of the criteria measured (i.e., sex ratios, developmental timing, and/or sex-specific mortality). Of course, there are limitations with the scope of the criteria measured as there could be other impacts missed, but these specific impacts were chosen with future applications in mind.

Based on these specific criteria, two binding partners of DSX^{F}, *DNA-directed RNA-polymerase subunit rpb8* (AAEL000677) and *WD repeat-containing protein 48 homolog* (AAEL021400), are of particular interest. *DNA-directed RNA-polymerase subunit rpb8* (herein referred to as *Rpb8*), demonstrated both significant larval mortality and a skewed sex-ratio, favouring male development – indicative of female-specific lethality. Furthermore, the binding-interaction of Rpb8 with both female-specific isoforms was confirmed through 1-on-1 pulldown experiments (Figure 9), and pupal proteome analysis (male versus female) confirmed a 4-fold higher expression of Rpb8 in females relative to males (Figure 14). As DSX acts as a transcription factor, it is not entirely unsurprising to find a DSX binding interaction with a subunit of the RNA polymerase complex, yet the sex-biased expression and dsRNA-mediated lethality is noteworthy. It is possible that the requirement for female mosquitoes to reach a larger, more complex adult form may necessitate higher levels of gene expression and thus the

association with Rpb8 is necessary. Furthermore, it is possible that DSX^M may associate with the RNA polymerase complex through a different interaction, thereby lowering its dependence on Rpb8 expression.

While the consumption of dsRNA targeting *Rpb8* resulted in female-biased lethality, significantly delayed female development was observed in assays targeting *WD repeat-containing protein 48 homolog* (herein referred to as *WD48*). Furthermore, a male-biased sex-ratio without an increase in larval mortality was observed. In a broad range of taxa, ranging from *Caenorhabditis elegans* (Dahlberg and Juo, 2014) to *Homo sapiens* (Hodul et al., 2020), WD48 homologs are known for their deubiquitination activity and involvement in processes related to proteolysis, cell cycle, and cell proliferation (Hodul et al., 2020; Li et al., 2022). Consequently, the slowed growth and development observed from the feeding of dsRNA specific to *wd48* could be explained by a decrease in cell proliferation activity. Notably, the role of WD48 in ubiquitination complexes could be of particular significance for DSX as it may interact with ubiquitin associated folds which are essential for dimerization (Bayrer et al., 2005). In *D. melanogaster*, it was postulated that ubiquitination machinery associated with DSX could be responsible for regulation of sex differentiation through several possible methods (Bayrer et al., 2005). Aside from a proteolytic regulatory pathway where each round of transcription is followed by degradation of the transcription factor, DSX ubiquitination could otherwise be responsible for mediating protein-protein interactions, subcellular localization, transcriptional activation, and/or mRNA processing (Bayrer et al., 2005). With the need for tight spaciotemporal regulation in sex-differentiation (Rice et al., 2019), the interaction between WD48 and DSX^F could be mediated through this ubiquitin associated fold and its potential regulatory significance (Bayrer et al., 2005).

A curious interaction identified in the mass-spectrometry analysis was between DSX^F and the protein Glutamate synthase (AAEL014768). While known only to be a cytosolic protein, this protein demonstrated a high degree of binding to both isoforms relative to negative controls, and furthermore produced significant impacts on all three criteria considered in the dsRNA feeding assays (i.e. female-specific impacts to developmental timing and mortality, as well as a skewed sex-ratio). Without the presence of a nuclear localization signal on Glutamate Synthase, it is likely that this finding was an artifact of cytosolic contamination in the nuclear lysate – however the strong ratio of binding to both DSX^F isoforms relative to controls led me to analyze this gene further. While a curious result, these findings from the dsRNA-feeding assays may still be applicable to an improved understanding of sex-development. It was recently demonstrated in *Daphnia pulex* that glutamatergic signalling was essential for male sex-development through its respective impact on sex-specific gene expression patterns (Camp et al., 2020). As homologs of *Doublesex*, *Sex lethal*, and *Transformer* are found in *Daphnia sp.,* the authors postulated that glutamatergic pathways may have an impact on the respective activity of these sex development proteins (Camp et al., 2020). Finally, the association between cytosolic proteins and DSX are not necessarily artifactual. In the lepidopteran *Zerene cesonia*, intracellular localization of DSX was highly regulated during wing development, demonstrating primarily cytosolic localization at 48h post pupation, and shifting to diffuse localization between the nucleus and cytosol at 72h post pupation (Rodriguez-Caro et al., 2021). This spatiotemporal, intracellular localization of DSX is likely an extra level of DSX regulation, controlled through an unknown mechanism (Rodriguez-Caro et al., 2021). While interactions with cytosolic proteins are unexpected and potentially artifactual, it is intriguing to consider the potential regulatory activity of the sex-specific oligomerization domains outside of a transcription factor complex.

4.3 Applications and optimization of female-specific developmental delay

Improved understanding of Doublesex isoforms and their binding partners in *Aedes aegypti* provides three clear benefits: 1) Improved resolution for the sex-differentiation pathway of an arbovirus vector, *Aedes aegypti*; 2) Tangential insights for insect sex-development processes in general; and 3) New targets for improved insect sex-sorting and/or female-specific lethality. With climate change expected to increase the range of disease vectors *Aedes aegypti* and its close relative *Aedes albopictus* to threaten half the world's population by 2050 (Kraemer et al., 2019), new methods of control are needed. Of particular interest are techniques involving the mass release of males either sterilized or infected with *Wolbachia sp* where they mate fruitlessly with wild females. Being pesticide-free population suppression methods, these techniques demonstrate high degrees of success when implemented correctly (Gato et al., 2021; Zabalou et al., 2004). Both techniques, however, rely on the effective and successful removal of females from the population (Lutrat et al., 2019). It is impossible to distinguish male and female larvae, and with the release of millions of male mosquitoes, impractical to sex sort pupae based on limited dimorphic features. Thus, a method of actively suppressing female development is needed. While transgenic methods of importing sex-sorting or inhibiting survival of mosquitoes have been developed (reviewed in Seirin Lee et al., 2013), public perception and regulatory processes related with GMO technologies present significant barriers to their adoption. Thus, an effective, non-transgenic sex-sorting process, such as the transient, RNAi-based strategies used in this study are worth considering. From this project, the feeding of dsRNA targeting several DSX^F binding partners demonstrated significant impacts to female development, ranging from altered developmental timing to larval/pupal mortality. While female-specific larval mortality

would be a most desirable outcome, as it could require up to 50% less resources to produce the same male population, the treatments from this project were never able to reach 100% female mortality, and furthermore some treatments demonstrated accelerated female development relative to males (Figure 11). A smaller interval between male and female development makes it significantly more difficult to reliably remove male pupae from a population, even compared to untreated controls. From this project, *WD48* (AAEL021400) would be the most useful gene to target for the purposes of sex sorting. By further delaying female-development relative to male emergence, it becomes possible to selectively remove male pupae within a predictable time interval without the risk of female contamination. Sex-exclusive proteins identified in the proteome analysis could additionally point to potential targets for female-specific lethality, which should be followed up in a further analysis. It would be interesting to compare differences in efficacy of genes showing a sex-bias compared to sex-exclusive expression for the purposes of improved mosquito sex-sorting. While proteins demonstrating female-exclusive expression may prove effective at specifically impacting female development, mortality, fecundity, or behaviour, their impact will largely depend on the timing of gene expression. For the purposes of improved sex-sorting, the ideal gene candidates for knockdown are those which demonstrate sex-biased or sex-exclusive expression in the early larval stages. Using these criteria, the mediating dsRNA molecules have longer times for impact, and in cases where female-lethal phenotypes are produced, fewer resources are required to rear the desired male-only population of mosquitoes.

To improve the efficacy of delayed female development using dsRNA targeting *WD48*, this project determined that a lower temperature significantly increases the interval between male and female pupation by an average of approximately 0.5 days. As the developmental timing of insects is delayed or accelerated by decreases or increases in temperature, respectively (Teng and

Apperson, 2000), this may provide a longer duration of time for *dsWD48* to impact female development, resulting in an improved developmental delay. This provides more time for the majority of male pupae to be collected without the risk of contaminating females.

This project made use of economical and simplistic dsRNA expression and delivery systems which would be practical for mass-rearing of male mosquitoes. Furthermore, for use in sterile insect technique approaches, it becomes possible to co-feed multiple bacterially produced dsRNAs targeting genes responsible for female development and male fertility. This would avoid the large doses of radiation used to sterilize males which can weaken their sexual competitiveness (Helinski and Knols, 2008). Such a system could greatly improve current techniques used in SIT for mosquitoes and have potential applications in controlling other insect pests.

5 CONCLUSIONS AND FUTURE DIRECTIONS

With identical DNA-binding domains, identification of isoform specific binding partners is an essential step to understanding the sex-specific, transcription factor activity of Doublesex. Protein pulldown followed by mass spectrometry techniques permitted the identification of 50 potential binding partners for the two female-specific isoforms, two of which were confirmed through subsequent pulldown assays. Furthermore, the dsRNA-mediated knockdown of eight of the selected targets identified in the mass-spectrometry assay resulted in significant impacts to development. From these assays, the deubiquitinating protein, WD48 was identified as having the most impactful knockdown phenotype for male-specific, sex-sorting applications, particularly when larvae were grown at room temperature. While mass-spectrometry and dsRNA-mediated knockdown provide evidence of this binding interaction, it is still necessary to provide confirmation, either through similar protein pulldown assays or a yeast-2-hybrid experiment. Furthermore, while only 12 of the mass-spectrometry targets were chosen for knockdown, further RNAi-mediated knockdown experiments should focus on the other prospective protein-binding partners identified.

This project further identified DSX^{F2} as the major female isoform expressed across development. The expression of both a major and minor isoform may pose an additional regulatory mechanism by which DSX can impact sexually dimorphic gene expression in a spatiotemporal manner. While far from conclusive, it is intriguing to consider that, of the targets chosen for knockdown, significant developmental impacts were identified following the knockdown of the two binding partners exclusive to DSX^{F2} whereas no significant impacts were observed after knockdown of the one DSX^{F1} binding partner tested. Future projects should

include isoform-specific dsRNA-mediated knockdown assays to better understand the relative impacts and importance of each isoform throughout development.

While this project identified a subset of genes expected to interact with DSX^{F1} and DSX^{F2}, their roles in activating or repressing transcriptional activity of a particular gene target remain unknown. Future projects should consider how the DSX-binding partner complexes function to regulate DSX activity, and additionally focus on the mechanisms guiding DSX spatiotemporal expression and intracellular localization. Furthermore, the binding partners of DSX^{M} will be identified in a following experiment.

WDR48 may prove useful in insect control programs where mass release of male-only populations is required. The further delayed development of female mosquitoes relative to male mosquitoes, in conjunction with traditional, high-throughput, pupal size-based sex-separation techniques would allow for a high degree of confidence in preventing contamination of female mosquitoes.

6 REFERENCES

Aryan, A., Anderson, M.A.E., Biedler, J.K., Qi, Y., Overcash, J.M., Naumenko, A.N., Sharakhova, M. V., Mao, C., Adelman, Z.N., Tu, Z., 2020. Nix alone is sufficient to convert female Aedes aegypti into fertile males and myo-sex is needed for male flight. Proc Natl Acad Sci U S A 117, 17702–17709. https://doi.org/10.1073/pnas.2001132117

Bayrer, J.R., Zhang, W., Weiss, M.A., 2005. Dimerization of Doublesex Is Mediated by a Cryptic Ubiquitin-associated Domain Fold. Journal of Biological Chemistry 280, 32989–32996. https://doi.org/10.1074/jbc.M507990200

Beye, M., Hasselmann, M., Fondrk, M.K., Page, R.E., Omholt, S.W., 2003. The gene csd is the primary signal for sexual development in the honeybee and encodes an SR-type protein. Cell 114, 419–429. https://doi.org/10.1016/S0092-8674(03)00606-8

Biedler, J.K., Tu, Z., 2016. Sex Determination in Mosquitoes. Adv In Insect Phys 51, 37–66. https://doi.org/10.1016/bs.aiip.2016.05.005

Blackmon, H., Ross, L., Bachtrog, D., 2017. Sex determination, sex chromosomes, and karyotype evolution in insects. Journal of Heredity 108, 78–93. https://doi.org/10.1093/jhered/esw047

Camp, A.A., Yun, J., Chambers, S.A., Haeba, M.H., LeBlanc, G.A., 2020. Involvement of glutamate and serotonin transmitter systems in male sex determination in Daphnia pulex. J Insect Physiol 121, 104015. https://doi.org/10.1016/j.jinsphys.2020.104015

Cho, S., Huang, Z.Y., Zhang, J., 2007. Sex-specific splicing of the honeybee doublesex gene reveals 300 million years of evolution at the bottom of the insect sex-determination pathway. Genetics 177, 1733–1741. https://doi.org/10.1534/genetics.107.078980

Christophers, S.R., 1960. Aëdes Aegypti (L.), the Yellow Fever Mosquito: Its Life History, Bionomics, and Structure. Cambridge University Press, Cambridge.

Clough, E., Jimenez, E., Kim, Y.A., Whitworth, C., Neville, M.C., Hempel, L.U., Pavlou, H.J., Chen, Z.X., Sturgill, D., Dale, R.K., Smith, H.E., Przytycka, T.M., Goodwin, S.F., VanDoren, M., Oliver, B., 2014. Sex- and tissue-specific functions of drosophila doublesex transcription factor target genes. Dev Cell 31, 761–773. https://doi.org/10.1016/j.devcel.2014.11.021

Dahlberg, C.L., Juo, P., 2014. The WD40-repeat Proteins WDR-20 and WDR-48 Bind and Activate the Deubiquitinating Enzyme USP-46 to Promote the Abundance of the Glutamate Receptor GLR-1 in the Ventral Nerve Cord of Caenorhabditis elegans. Journal of Biological Chemistry 289, 3444–3456. https://doi.org/10.1074/jbc.M113.507541

De La Filia, A.G., Bain, S.A., Ross, L., 2015. Haplodiploidy and the reproductive ecology of Arthropods. Curr Opin Insect Sci 9, 36–43. https://doi.org/10.1016/j.cois.2015.04.018

Deshmukh, R., Lakhe, D., Kunte, K., 2020. Tissue-specific developmental regulation and isoform usage underlie the role of *doublesex* in sex differentiation and mimicry in *Papilio* swallowtails. R Soc Open Sci 7, 200792. https://doi.org/10.1098/rsos.200792

Dübendorfer, A., Hediger, M., Burghardt, G., Bopp, D., 2002. Musca domestica, a window on the evolution of sex-determining mechanisms in insects. International Journal of Developmental Biology 46, 75–79. https://doi.org/10.1387/ijdb.11902690

Duman-Scheel, M., Syed, Z., 2015. Developmental neurogenetics of sexual dimorphism in Aedes aegypti. Front Ecol Evol 3, 1–8. https://doi.org/10.3389/fevo.2015.00061

Gardner, A., Ross, L., 2014. Mating ecology explains patterns of genome elimination. Ecol Lett 17, 1602–1612. https://doi.org/10.1111/ele.12383

Gato, R., Menéndez, Z., Prieto, E., Argilés, R., Rodríguez, M., Baldoquín, W., Hernández, Y., Pérez, D., Anaya, J., Fuentes, I., Lorenzo, C., González, K., Campo, Y., Bouyer, J., 2021. Sterile Insect Technique: Successful Suppression of an Aedes aegypti Field Population in Cuba. Insects 12, 469. https://doi.org/10.3390/insects12050469

Hall, A.B., Basu, S., Jiang, X., Qi, Y., Timoshevskiy, V.A., Biedler, J.K., Sharakhova, M. V., Elahi, R., Anderson, M.A.E., Chen, X.G., Sharakhov, I. V., Adelman, Z.N., Tu, Z., 2015. A male-determining factor in the mosquito Aedes aegypti. Science (1979) 348, 1268–1270. https://doi.org/10.1126/science.aaa2850

Harker, B.W., Behura, S.K., Debruyn, B.S., Lovin, D.D., Mori, A., Romero-Severson, J., Severson, D.W., 2013. Stage-specific transcription during development of Aedes aegypti. BMC Dev Biol 13. https://doi.org/10.1186/1471-213X-13-29

Helinski, M.E.H., Knols, B.G.J., 2008. Mating Competitiveness of Male *Anopheles arabiensis* Mosquitoes Irradiated with a Partially or Fully Sterilizing Dose in Small and Large Laboratory Cages. J Med Entomol 45, 698–705. https://doi.org/10.1093/jmedent/45.4.698

Hodul, M., Ganji, R., Dahlberg, C.L., Raman, M., Juo, P., 2020. The WD40-repeat protein WDR-48 promotes the stability of the deubiquitinating enzyme USP-46 by inhibiting its ubiquitination and degradation. Journal of Biological Chemistry 295, 11776–11788. https://doi.org/10.1074/jbc.RA120.014590

Jin, B., Zhao, Y., Dong, Y., Liu, P., Sun, Y., Li, X., Zhang, X., Chen, X., Gu, J., 2021. Alternative splicing patterns of *doublesex* reveal a missing link between *Nix* and *doublesex* in the sex determination cascade of *Aedes albopictus*. Insect Sci 28, 1601–1620. https://doi.org/10.1111/1744-7917.12886

Kiuchi, T., Koga, H., Kawamoto, M., Shoji, K., Sakai, H., Arai, Y., Ishihara, G., Kawaoka, S., Sugano, S., Shimada, T., Suzuki, Y., Suzuki, M.G., Katsuma, S., 2014. A single female-specific piRNA is the primary determiner of sex in the silkworm. Nature 509, 633–636. https://doi.org/10.1038/nature13315

Kopp, A., 2012. Dmrt genes in the development and evolution of sexual dimorphism. Trends in Genetics 28, 175–184. https://doi.org/10.1016/j.tig.2012.02.002

Kraemer, M.U.G., Reiner, R.C., Brady, O.J., Messina, J.P., Gilbert, M., Pigott, D.M., Yi, D., Johnson, K., Earl, L., Marczak, L.B., Shirude, S., Davis Weaver, N., Bisanzio, D., Perkins, T.A., Lai, S., Lu, X., Jones, P., Coelho, G.E., Carvalho, R.G., Van Bortel, W., Marsboom, C., Hendrickx, G., Schaffner, F., Moore, C.G., Nax, H.H., Bengtsson, L., Wetter, E., Tatem, A.J., Brownstein, J.S., Smith, D.L., Lambrechts, L., Cauchemez, S., Linard, C., Faria, N.R., Pybus, O.G., Scott, T.W., Liu, Q., Yu, H., Wint, G.R.W., Hay, S.I., Golding, N., 2019. Past and future spread of the arbovirus vectors Aedes aegypti and Aedes albopictus. Nat Microbiol 4, 854–863. https://doi.org/10.1038/s41564-019-0376-y

Krzywinska, E., Dennison, N.J., Lycett, G.J., Krzywinski, J., 2016. A maleness gene in the malaria mosquito Anopheles gambiae. Science (1979) 353, 67–69. https://doi.org/10.1126/science.aaf5605

Krzywinska, E., Ferretti, L., Li, J., Li, J.-C., Chen, C.-H., Krzywinski, J., 2021. femaleless Controls Sex Determination and Dosage Compensation Pathways in Females of Anopheles Mosquitoes. Current Biology 31, 1084-1091.e4. https://doi.org/10.1016/j.cub.2020.12.014

Ledón-Rettig, C.C., Zattara, E.E., Moczek, A.P., 2017. Asymmetric interactions between doublesex and tissue-and sex-specific target genes mediate sexual dimorphism in beetles. Nat Commun 8, 1–10. https://doi.org/10.1038/ncomms14593

Lehane, M., 2005. The Biology of Blood-Sucking Insects, Second. ed. Cambridge University Press, New York.

Li, B., Zhang, Y., Cao, K., Li, C., Chen, Q., Jiang, Y., Luo, L., Zuo, S., 2022. <scp>WD</scp> repeat domain 48 promotes hepatocellular carcinoma progression by stabilizing <scp>c-Myc</scp>. J Cell Mol Med 26, 5755–5766. https://doi.org/10.1111/jcmm.17583

Li, M., Yang, T., Kandul, N.P., Bui, M., Gamez, S., Raban, R., Bennett, J., Sánchez C., H.M., Lanzaro, G.C., Schmidt, H., Lee, Y., Marshall, J.M., Akbari, O.S., 2019. Development of a Confinable Gene-Drive System in the Human Disease Vector, Aedes aegypti. bioRxiv 1–22. https://doi.org/10.1101/645440

Liu, P., Jin, B., Li, X., Zhao, Y., Gu, J., Biedler, J.K., Tu, Z.J., Chen, X.G., 2020. Nix is a male-determining factor in the Asian tiger mosquito Aedes albopictus. Insect Biochem Mol Biol 118, 103311. https://doi.org/10.1016/j.ibmb.2019.103311

Lutrat, C., Giesbrecht, D., Marois, E., Whyard, S., Baldet, T., Bouyer, J., 2019. Sex Sorting for Pest Control: It's Raining Men! Trends Parasitol 35, 649–662. https://doi.org/10.1016/j.pt.2019.06.001

Magnusson, K., Mendes, A.M., Windbichler, N., Papathanos, P.A., Nolan, T., Dottorini, T., Rizzi, E., Christophides, G.K., Crisanti, A., 2011. Transcription regulation of sex-biased genes during ontogeny in the Malaria vector Anopheles gambiae. PLoS One 6. https://doi.org/10.1371/journal.pone.0021572

Mysore, K., Sun, L., Tomchaney, M., Sullivan, G., Adams, H., Piscoya, A.S., Severson, D.W., Syed, Z., Duman-Scheel, M., 2015. siRNA-Mediated Silencing of doublesex during Female Development of the Dengue Vector Mosquito Aedes aegypti. PLoS Negl Trop Dis 9, 1–21. https://doi.org/10.1371/journal.pntd.0004213

Penalva, L.O.F., Sánchez, L., 2003. RNA Binding Protein Sex-Lethal (Sxl) and Control of Drosophila Sex Determination and Dosage Compensation. Microbiology and Molecular Biology Reviews 67, 343–359. https://doi.org/10.1128/mmbr.67.3.343-359.2003

Price, D.C., Egizi, A., Fonseca, D.M., 2015a. The ubiquity and ancestry of insect doublesex. Sci Rep 5, 13068. https://doi.org/10.1038/srep13068

Price, D.C., Egizi, A., Fonseca, D.M., 2015b. Characterization of the doublesex gene within the Culex pipiens complex suggests regulatory plasticity at the base of the mosquito sex determination cascade. BMC Evol Biol 15, 108. https://doi.org/10.1186/s12862-015-0386-1

Rice, G.R., Barmina, O., Luecke, D., Hu, K., Arbeitman, M., Kopp, A., 2019. Modular tissue-specific regulation of doublesex underpins sexually dimorphic development in drosophila. Development (Cambridge) 146, 1–11. https://doi.org/10.1242/dev.178285

Rodriguez-Caro, F., Fenner, J., Bhardwaj, S., Cole, J., Benson, C., Colombara, A.M., Papa, R., Brown, M.W., Martin, A., Range, R.C., Counterman, B.A., 2021. Novel *Doublesex* Duplication Associated with Sexually Dimorphic Development of Dogface Butterfly Wings. Mol Biol Evol 38, 5021–5033. https://doi.org/10.1093/molbev/msab228

Rose, G., Krzywinska, E., Kim, J., Revuelta, L., Ferretti, L., Krzywinski, J., 2016. Dosage compensation in the African malaria mosquito *Anopheles gambiae*. Genome Biol Evol evw004. https://doi.org/10.1093/gbe/evw004

Salvemini, M., Mauro, U., Lombardo, F., Milano, A., Zazzaro, V., Arcà, B., Polito, L.C., Saccone, G., 2011. Genomic organization and splicing evolution of the doublesex gene, a Drosophila regulator of sexual differentiation, in the dengue and yellow fever mosquito Aedes aegypti. BMC Evol Biol 11, 41. https://doi.org/10.1186/1471-2148-11-41

Salz, H.K., Erickson, J.W., 2010. Sex determination in Drosophila: The view from the top. Fly (Austin) 4, 60–70. https://doi.org/10.4161/fly.4.1.11277

Sanchez-Bayo, F., A., H., Gok, K., 2013. Impact of Systemic Insecticides on Organisms and Ecosystems, in: Insecticides - Development of Safer and More Effective Technologies. InTech. https://doi.org/10.5772/52831

Scudder, G.G.E., 2009. The Importance of Insects. Insect Biodiversity: Science and Society 7–32. https://doi.org/10.1002/9781444308211.ch2

Seirin Lee, S., Baker, R.E., Gaffney, E.A., White, S.M., 2013. Modelling Aedes aegypti mosquito control via transgenic and sterile insect techniques: Endemics and emerging outbreaks. J Theor Biol 331, 78–90. https://doi.org/10.1016/j.jtbi.2013.04.014

Shukla, J.N., Palli, S.R., 2012. Sex determination in beetles: Production of all male progeny by Parental RNAi knockdown of transformer. Sci Rep 2. https://doi.org/10.1038/srep00602

Teng, H.-J., Apperson, C.S., 2000. Development and Survival of Immature *Aedes albopictus* and *Aedes triseriatus* (Diptera: Culicidae) in the Laboratory: Effects of Density, Food, and Competition on Response to Temperature. J Med Entomol 37, 40–52. https://doi.org/10.1603/0022-2585-37.1.40

Tomchaney, M., Mysore, K., Sun, L., Li, P., Emrich, S.J., Severson, D.W., Duman-Scheel, M., 2014. Examination of the genetic basis for sexual dimorphism in the Aedes aegypti (dengue vector mosquito) pupal brain. Biol Sex Differ 5, 1–22. https://doi.org/10.1186/s13293-014-0010-x

Verhulst, E.C., 2010. Maternal control of haplodiploid sex. Science (1979) 328, 620–623.

Verhulst, E.C., van de Zande, L., Beukeboom, L.W., 2010. Insect sex determination: It all evolves around transformer. Curr Opin Genet Dev 20, 376–383. https://doi.org/10.1016/j.gde.2010.05.001

Whyard, S., Erdelyan, C.N.G., Partridge, A.L., Singh, A.D., Beebe, N.W., Capina, R., 2015. Silencing the buzz: A new approach to population suppression of mosquitoes by feeding larvae double-stranded RNAs. Parasit Vectors 8, 1–11. https://doi.org/10.1186/s13071-015-0716-6

Zabalou, S., Riegler, M., Theodorakopoulou, M., Stauffer, C., Savakis, C., Bourtzis, K., 2004. *Wolbachia* -induced cytoplasmic incompatibility as a means for insect pest population control. Proceedings of the National Academy of Sciences 101, 15042–15045. https://doi.org/10.1073/pnas.0403853101

Zhang, H., Lui, R., 2020. Releasing Wolbachia-infected Aedes aegypti to prevent the spread of dengue virus: A mathematical study. Infect Dis Model 5, 142–160. https://doi.org/10.1016/j.idm.2019.12.004

7 APPENDIX

Table A1. Primers used for this study. 5' restriction sites underlined

Gene Name	Accession	Primer Type	Sequence 5' – 3'
40S ribosomal protein S7	AAEL009496, XM_001660119.2	qPCR	*F: CCATTGAACACAAGGTCGACAC* *R: GTAGGGCTCCGGGAATTCGA*
Nix	AAEL022912, XM_021851185.1	qPCR	*F: CGCTCTATTGGAATATTTGGATTGC* *R: TGAATGTCGCCAAACCTTGA*
Doublesex (Generic)	AAEL009114	qPCR	*F: CTGTCAACCTCCGAGAGGGTA* *R:TGTTGGCGTGAAACCTTCGT*
Doublesex (Male)	AAEL009114, NM_001358381.1	qPCR	*F: ACGGATTGACGAAGGATACGA* *R: GGGTGACGGAGATGTTCTCCT*
		CDS (pYES)	*F: AAAAAGCTTATGGTTTCGCAAGATCGCTG* *R: AAATCTAGAGTGAATCGACGCAACGGG*
		CDS (pBAD)	*F: AAACCATGGTTTCGCAAGATCGCTG* *R: AAAAAGCTTGTGAATCGACGCAACGGG*
Doublesex (Female Isoform 1)	AAEL009114, NM_001358382.1	qPCR	*F: CCAACGGATTGACGAAGGTCAAG* *R: TACTGCGCAACTCTACACCGT*
		CDS (pYES)	*F: AAAAAGCTTATGGTTTCGCAAGATCGCTG* *R: AAATCTAGATCCGGACTGGCGCGTCGTA*
		CDS (pBAD)	*F: AAACCATGGTTTCGCAAGATCGCTG* *R: AAAAAGCTTTCCGGACTGGCGCGTCGTA*
Doublesex (Female Isoform 2)	AAEL009114, NM_001358383.1	qPCR	*F: AACGGATTGACGAAGTGCAA* *R: AGGAACGCTGTCTCACAAGT*
		CDS (pYES)	*F: AAAAAGCTTATGGTTTCGCAAGATCGCTG* *R: AAATCTAGACACGTGGTAGCCCCAGAAT*
		CDS (pBAD)	*F: AAACCATGGTTTCGCAAGATCGCTG* *R: AAAAAGCTTCACGTGGTAGCCCCAGAAT*
DNA-directed RNA polymerase subunit rpb8	AAEL000677, XM_001649743.2	CDS (pGEX)	*F: AAAAAACTCGAGATGTCCGGAATTCTGTTTGA* *R: AAAAAACTCGAGCTAGAAAGCCAACTTCTTCA*
		dsRNA	*F: AAAAAACTCGAGACATGGATCCGGAAGGCAAG* *R: AAAAAATCTAGAGTAATCCGCCGAACGAAACG*
mRNA cap guanine-N7 methyltransferase	AAEL021810, XM_021856968.1	CDS (pGEX)	*F: AAAAAAGAATTCTTCGCCGCTGACGCCACA* *R:AAAAAAGAATTCTTACGAATAGACAGGTTTTCCC*
		dsRNA	*F: GTGATGGACATGTGTTGCGG*

			R: CATTCGGCGGCATTCTTCAG
Nop14	AAEL014051, XM_001657290.2	dsRNA	*F: TGAGCTGCCTCGAAAGTACG* *R: TGGAGTTACAACGGGATGGC*
WD repeat-containing protein 48	AAEL021400 XM_021840350.1	dsRNA	*F: CATTAAGGGTGGAGCTGCGA* *R: CGTCGCATCCGTTTGAATCC*
CAF1C_H4-bd domain-containing protein	AAEL027479, XM_001660533.2	dsRNA	*F: AAAAAACTCGAGCGTTTATGGTGGCTGGGACT* *R: AAAAAATCTAGAAAAATCCGGCTTCACTCCGT*
Zinc finger protein	AAEL010847, XM_001661028.1	dsRNA	*F: AAAAAACTCGAGCCGAAGCGATACAAACGCAG* *R: AAAAAATCTAGATTCGCCATTTGGCTGTTGTG*
PWI domain-containing protein	AAEL023022, XM_021838104.1	dsRNA	*F: AAAAAACTCGAGCCCATCGAGTCCGATTCCAG* *R: AAAAAATCTAGATCTTGGCGTTTGCGTTCAAG*
Aspartyl-tRNA synthetase	AAEL011655, XM_001661774.1	dsRNA	*F: AAAAAACTCGAGAGGAAGCCATCCACGTTCTG* *R: AAAAAATCTAGAGTCGGGACCGATCCAAACTT*
Aminoacyl-tRNA synthetase auxiliary protein	AAEL010514, XM_001650634.1	dsRNA	*F: AAAAAACTCGAGCTGCGAAAACAGGTGGAAGC* *R: AAAAAATCTAGACGACCAACGTCTATCGGAGG*
Succinyl-CoA ligase beta subunit	AAEL011746, XM_001661816.1	dsRNA	*F: AAAAAACTCGAGCGGCAAGATGATCAAGCAGC* *R: AAAAAATCTAGACTCCAGCATCCTCGGCATAG*
SEC63	AAEL025151, XM_021857125.1	dsRNA	*F: AAAAAACTCGAGAGAATGTCAGTGCGAACCGT* *R: AAAAAATCTAGAGAGCAATGCCGAACGATGTC*
Glutamate synthase	AAEL014768, XM_021841419.1	dsRNA	*F: AAAAAACTCGAGGAATTCGGATTCAGCACGGC* *R: AAAAAATCTAGATGGGCGAAGATCCAAAGCAT*

Table A2. Coding sequences for recombinant proteins

Fusion Protein	Accession (VEuPathDB, NCBI)	Sequence (5' – 3')
6His-DSX^{F1}	AAEL009114, NM_001358382.1	ATGGTTTCGCAAGATCGCTGGATGGTAAAGATGTCCGAGGCAGGGTACG ATAACCGGGCGGATGGCAGTGGAGCTTCCAGCAGCAGCCTGAACCCGCG AACGCCGCCGAACTGTGCCCGCTGCCGGAACCACGGTCACAAGATCGGC CTGAAGGGACGCAAGCGCTATTGTAAGTATCGCAATTGTACCTGCGAAA AGTGCTGCCTGACGGCCGAACGGCAGCGGGTCATGGCCCTGCAGACGGC TCTCCGAAGGGCGCAAACCCAGGACGAACAGCGGTTGCTGGTAGACGGA GAGGTGCCCGCCGAACCGCAGAGGTCGTTGATCGACTGCGACTCGTCCA GCGGCTCGATGAACTCCACCCCGGGCAGCTCGTTGGTAACGCTGTCCCAG CACCGAAGATCACCCTGCTCCGCCGCGTCGGTCCACCCCAGCGAGGCTCA GCAAAACGTTGCAGCCAACCACTCCAGCGGAACCCCTGAACCCGGAAAC ATGGTACCAGTTGGCCCCCATATGCGAGTGCAGCATCACGGACCGGACTC AGGAGCAGACGACGAACTTGTCAAACGATCTCAATGGCTGCTGGAGAAG CTACGATACCCCTGGGAGATGATGCCCCTGATGTACGTGATACTGAAAGG CGCCGACGGAGACGTCAATAAAGCGCGCCAACGGATTGACGAAGGTCAA GCCGTGGTCAATGAATACTCACGATTGCACAATCTGAACATGTTCGACGG TGTGGAGTTGCGCAGTACGACGCGCCAGTCCGGAAAGCTTGGGCCCGAA CAAAAACTCATCTCAGAAGAGGATCTGAATAGCGCCGTCGACCATCATC ATCATCATCATTGA
6His-DSX^{F2}	AAEL009114, NM_001358383.1	ATGGTTTCGCAAGATCGCTGGATGGTAAAGATGTCCGAGGCAGGGTACG ATAACCGGGCGGATGGCAGTGGAGCTTCCAGCAGCAGCCTGAACCCGCG AACGCCGCCGAACTGTGCCCGCTGCCGGAACCACGGTCACAAGATCGGC CTGAAGGGACACAAGCGCTATTGTAAGTATCGCAATTGTACCTGCGAAA AGTGCTGCCTGACGGCCGAACGGCAGCGGGTCATGGCCCTGCAGACGGC TCTCCGAAGGGCGCAAACCCAGGACGAACAGCGGTTGCTGGTAGACGGA GAGGTGCCCGCCGAACCGGTACACAGCCTTCAAATACCAAAATTGTCTG ACCTAAAAGAGATGATCCATAATTCTCAGCAGAGGTCGTTGATCGACTGC GACTCGTCCACCGGCTCGATGAACTCCACCCCGGGCAGCTCGTTGGTAAC GCTGTCCCAGCACCGAAGATCACCCTGCTCCGCCGCGTCGGTCCACCCCA GCGAGGCTCAGCAAAACGTTGCAGCCAACCACTCCAGCGGAACCCCTGA ACCCGGAAACATGGTACCAGTTGGCCCCCATATGCGAGTGCAGCATCAC GGACCGGACTCAGGAACAGACGACGAACTTGTCAAACGATCTCAATGGC TGCTGGAGAAGCTGCGATACCCCTGGGAGATGATGCCCCTGATGTACGTG ATACTGAAAGGCGCCGACGGAGACGTCAATAAAGCGCGCCAACGGATTG ACGAAGTGCAAATGCTGTTTAACGATAATAGCGACATGCAGCCATTCTGG GGCTACCACGTGAAGCTTGGGCCCGAACAAAAACTCATCTCAGAAGAGG ATCTGAATAGCGCCGTCGACCATCATCATCATCATTGA
GST-677	AAEL000677, XM_001649743.2	ATGTCCCCTATACTAGGTTATTGGAAAATTAAGGGCCTTGTGCAACCCAC TCGACTTCTTTTGGAATATCTTGAAGAAAAATATGAAGAGCATTTGTATG AGCGCGATGAAGGTGATAAATGGCGAAACAAAAAGTTTGAATTGGGTTT GGAGTTTCCCAATCTTCCTTATTATATTGATGGTGATGTTAAATTAACACA GTCTATGGCCATCATACGTTATATAGCTGACAAGCACAACATGTTGGGTG GTTGTCCAAAAGAGCGTGCAGAGATTTCAATGCTTGAAGGAGCGGTTTTG GATATTAGATACGGTGTTTCGAGAATTGCATATAGTAAAGACTTTGAAAC TCTCAAAGTTGATTTTCTTAGCAAGCTACCTGAAATGCTGAAAATGTTCG AAGATCGTTTATGTCATAAAACATATTTAAATGGTGATCATGTAACCCAT CCTGACTTCATGTTGTATGACGCTCTTGATGTTGTTTTATACATGGACCCA ATGTGCCTGGATGCGTTCCCAAAATTAGTTTGTTTTAAAAAACGTATTGA AGCTATCCCACAAATTGATAAGTACTTGAAATCCAGCAAGTATATAGCAT GGCCTTTGCAGGGCTGGCAAGCCACGTTTGGTGGTGGCGACCATCCTCCA AAATCGGATCTGGAAGTTCTGTTCCAGGGGCCCCTGGGATCCCCGGAATT CCCGGGTCGACTCGAGATGTCCGGAATTCTGTTTGAGGACATCTTCAACG TCAAGGACATGGATCCGGAAGGCAAGAAATTCGACCGTGCCAGCCGGTT ACACTGTGAATCGGAGTCCTTCAAAATGGACCTGATTCTGGACATCAACT CTTGGCTGTACCCGATGGAGCTGGGGGACAAATTCCGTCTGGTTTTGGCC

		ACGACTCTGCACGAAGATGGAACACCTGCAAGTATGGAGTACAATGCCG CGGAAATCGAGGGATCCCGTGCGGACAGTTTCGAGTACGTAATGTTCGG GAAGGTTTACCGGATCGAAGGAGATGACGCTCAGCTGGAATCGGCCAAC AGACTTTCGGCATACGTTTCGTTCGGCGGATTACTGATGCGACTCCAGGG CGACGCCAACAATCTGCACGGCTTCGAAATCGATCAGCACATGTACTTGC TGATGAAGAAGTTGGCTTTCTAG
GST-810	AAEL021810, XM_021856968.1	ATGTCCCCTATACTAGGTTATTGGAAAATTAAGGGCCTTGTGCAACCCAC TCGACTTCTTTTGGAATATCTTGAAGAAAAATATGAAGAGCATTTGTATG AGCGCGATGAAGGTGATAAATGGCGAAACAAAAAGTTTGAATTGGGTTT GGAGTTTCCCAATCTTCCTTATTATATTGATGGTGATGTTAAATTAACACA GTCTATGGCCATCATACGTTATATAGCTGACAAGCACAACATGTTGGGTG GTTGTCCAAAAGAGCGTGCAGAGATTTCAATGCTTGAAGGAGCGGTTTTG GATATTAGATACGGTGTTTCGAGAATTGCATATAGTAAAGACTTTGAAAC TCTCAAAGTTGATTTTCTTAGCAAGCTACCTGAAATGCTGAAAATGTTCG AAGATCGTTTATGTCATAAAACATATTTAAATGGTGATCATGTAACCCAT CCTGACTTCATGTTGTATGACGCTCTTGATGTTGTTTTATACATGGACCCA ATGTGCCTGGATGCGTTCCCAAAATTAGTTTGTTTTAAAAAACGTATTGA AGCTATCCCACAAATTGATAAGTACTTGAAATCCAGCAAGTATATAGCAT GGCCTTTGCAGGGCTGGCAAGCCACGTTTGGTGGTGGCGACCATCCTCCA AAATCGGATCTGGAAGTTCTGTTCCAGGGGCCCCTGGGATCCCCGGAATC CGAATTCTTCGCCGCTGACGCCACACTTCAACGGCTGAGGGAAAAGTACC GGGATCCGTCGATTGACCTCCATCTGGTCAGTTGCCAGTTCGCGTTCCAC TATTGCTTCGAATCGCTCAAACAGGCCGAGTTCATGCTGAAGAATGCCGC CGAATGCTTGAAGGAGGGTGGATACTTTATCGGGACCATTCCGGATGCG AACGAGATCATGAAACGGCAACGGGCAGCCGGAGGCGACAGCTTCGGG AACGATGTGTACAAGATTTCCTTCTTGTGCGACACGGAGAAGCCTCCGCT CTTCGGGGCTAAGTACAACTTCCAGCTGGACGGAGTCGTCGATTGTCCGG AGTTCCTGGTCCACTTCCCGACACTGGTAAAGCTGGCCCTCAAGTTTGGC CTCCGGCTGGTGGAGAAGAAACGGTTCGACGAGTTCTACGAGGAATCGG TTTCCAGTGGGCGCGGACTGCTCGAGAAGATGCAAGCGCTCGAAACGTT CCCGGGCTTCTCGAGGGATGACCGCGAGCGGCAGCAGAACCGGGAAGAG TACCGACACGCCCAGCAGTATCTGGACCGGAAGGACGGACGCCACACCA AGGTCGGGACGCTGTCCAAGTCGGAGTGGGAAGCTAGCACTTTGTACAT GTTCTTCGCTTTCCAGAAGATGAAAAAATCATGGGATAAGGAGGGAAAA CCTGTCTATTCGTAA

Table A3. Identified DSX^{F1} / DSX^{F2} binding partners from mass spectrometry analysis

Accession, (Uniprot, VEuPathDB)	Description	Molecular Function	DSX^{F1} Pulldown / Background	DSX^{F2} Pulldown / Background
Q16P83, AAEL011746	Succinate-CoA ligase subunit beta	Other molecular function	115.16	125.33
A0A1S4FI59, AAEL025151	SEC63 protein		69.06	124.78
A0A6I8TQA0, AAEL014768	Glutamate synthase (NADH)	Other molecular function	76.11	78.33
A0A6I8U5Z1, AAEL025555	Uncharacterized protein	Other molecular function	1.64	29.37
Q17CL6, AAEL004527	mRpS7		8.45	8.74
A0A6I8U3U9, AAEL025807	Uncharacterized protein	Other molecular function	9.72	8.25
A0A6I8U337, AAEL025078	Protein SEC13 homolog	Other molecular function	7.53	6.54
Q16KR2, AAEL012902	Heterogeneous nuclear ribonucleoprotein		0.53	6.26
A0A1S4FWI2, AAEL012582	rRNA adenine N(6)-methyltransferase	Nucleic acid binding activity; other molecular function	12.30	5.90
A0A6I8TQ91, AAEL014959	Heterogeneous nuclear ribonucleoprotein k	Nucleic acid binding activity	3.05	5.60
A0A6I8TM72, AAEL020553	Uncharacterized protein	Other molecular function	0.41	5.29
A0A6I8U8Y2, AAEL027479	CAF1C_H4-bd domain-containing protein		8.83	5.15
Q17GJ0, AAEL003001	WD repeat protein		4.98	4.03
Q0IEK2, AAEL009653	40S ribosomal protein S30	Other molecular function	4.45	3.87
A0A6I8U1M0, AAEL022687	Cas1_AcylT domain-containing protein	Other molecular function	0.00	3.56
A0A1S4FIM3, AAEL008099	Procollagen-lysine 5-dioxygenase	Other molecular function	1.19	3.40

A0A6I8TC56, AAEL005992	Adam (a disintegrin and metalloprotease)	Other molecular function	4.46	3.39
Q17AI3, AAEL010514	Aminoacyl-tRNA synthetase auxiliary protein, 43 kDa putative	Nucleic acid binding activity	0.00	3.32
A0A1S4FUB6, AAEL021810	mRNA cap guanine-N7 methyltransferase	Nucleic acid binding activity; other molecular function	3.51	3.01
Q16Q09, AAEL011458	Uncharacterized protein	Other molecular function	7.70	2.99
Q1HR05, AAEL009275	Serine/threonine-protein phosphatase	Other molecular function	1.98	2.75
A0A1S4FI67, AAEL008006	3-hydroxyacyl-coa dehyrogenase	Other molecular function	0.00	2.66
Q1HQM8, AAEL014325	26S proteasome regulatory complex subunit RPN5/PSMD12		0.07	2.50
Q17GH9, AAEL003011	NADH dehydrogenase, putative		1.45	2.39
A0A1S4G159, AAEL014051	Nop14		1.69	2.33
A0A1S4FU48, AAEL011764	Prophenoloxidase	Other molecular function	10.35	2.25
Q17NL0, AAEL000677	DNA-directed RNA polymerase subunit RPABC3		3.15	2.25
Q16PG0, AAEL011655	Asparagine--tRNA ligase	Nucleic acid binding activity; other molecular function	1.11	2.18
A0A1S4FVU5, AAEL012167	Elongation factor Tu	Nucleic acid binding activity; other molecular function	2.48	2.17
Q16RP1, AAEL010896	WD40 repeat-containing protein, SMU1		0.00	2.12
A0A1S4FKX7, AAEL008970	Uncharacterized protein	Other molecular function	0.00	2.00
A0A1S4FXE2, AAEL012715	Uncharacterized protein		0.00	1.91
Q17FC3, AAEL003469	NHP2 Protein		1.96	1.83
Q16MY0, AAEL021400	WD repeat-containing protein 48 homolog	Other molecular function	0.00	1.77

A0A6I8TWN0, AAEL019777	B30.2/SPRY domain-containing protein	Gene expression	2.33	1.74
A0A6I8TK08, AAEL010826	Histone-lysine n-methyltransferase	Nucleic acid binding activity; Methyltransferase activity	2.82	1.63
Q1HRT6, AAEL002534	60S ribosomal protein L10	Other molecular function	1.36	1.61
A0A1S4FSN6, AAEL011090	Complement component	Chromatin remodelling	1.21	1.41
Q17PV7, AAEL000210	Ribosomal protein L2	Other molecular function	1.26	1.39
J9EAK6, AAEL017293	Uncharacterized protein		2.93	1.35
Q17KM8, AAEL001616	Vesicle-fusing ATPase	Other molecular function	0.72	1.35
A0A6I8TY49, AAEL020116	DUF1713 domain-containing protein		3.39	1.31
A0A6I8T7P8, AAEL005170	Cytochrome c oxidase subunit 4	Transporter activity	2.74	1.04
Q16FA2, AAEL014847	Innexin		3.77	0.23
A0A1S4EUY3, AAEL000101	AMP dependent CoA ligase		3.08	0.12
A0A1S4F6S3, AAEL004137	Acyl-CoA dehydrogenase	Other molecular function	10.88	0.10
A0A6I8TPE4, AAEL014957	RNA-polymerase II-associated protein 3-like C-terminal domain-containing protein	Protein binding	12.60	0.00
Q16RV2, AAEL010847	Zinc finger protein	Nucleic acid binding activity	5.43	0.00
A0A1S4EWI6, AAEL000671	Toll-like receptor (TOLL6)	Other molecular function	4.64	0.00
A0A6I8TG30, AAEL014340	Uncharacterized protein	Other molecular function	3.66	0.00

Table A4. DsRNA sequences

Gene Target	Accession (VEuPathDB, NCBI)	Sequence (5' – 3')
DNA-directed RNA polymerase subunit rpb8	AAEL000677, XM_001649743.2	ACAUGGAUCCGGAAGGCAAGAAAUUCGACCGUGCCAG CCGGUUACACUGUGAAUCGGAGUCCUUCAAAAUGGAC CUGAUUCUGGACAUCAACUCUUGGCUGUACCCGAUGG AGCUGGGGGACAAAUUCCGUCUGGUUUUGGCCACGAC UCUGCACGAAGAUGGAACACCUGCAAGUAUGGAGUAC AAUGCCGCGGAAAUCGAGGGAUCCCGUGCGGACAGUU UCGAGUACGUAAUGUUCGGGAAGGUUUACCGGAUCGA AGGAGAUGACGCUCAGCUGGAAUCGGCCAACAGACUU UCGGCAUACGUUUCGUUCGGCGGAUUAC
mRNA cap guanine-N7 methyltransferase	AAEL021810, XM_021856968.1	GUGAUGGACAUGUGUUGCGGCAAGGGAGGAGACUUGC UCAAGUGGAUCAAGGGCAAUAUUACGCAUCUGAUUUG CACGGAUAUCGCGGAAGUUAGCGUUGAACAGUGCGAG GCCAGAUACAACAACAUCAACCAGAAAAACGAUCAGG GCGGGAAGCCGUUUACGGCAGAAUUCUUCGCCGCUGA CGCCACACUUCAACGGCUGAGGGAAAAGUACCGGGAU CCGUCGAUUGACCUCCAUCUGGUCAGUUGCCAGUUCG CGUUCCACUAUUGCUUCGAAUCGCUCAAACAGGCCGA GUUCAUGCUGAAGAAUGCCGCCGAAUG
Nop14	AAEL014051, XM_001657290.2	UGAGCUGCCUCGAAAGUACGAACAGUUGGAAGAACUA CUGCAGCGACGAUCAUCGGCAGAACAACUCGUCAUAC UUGAUAGAAUGGUUAAGUCAAACAAUGCAAAGUUUUC UCGCGAAAACAAACAAAAAAUGGUGUCGCUUUAUGCA UUUUUGCUUCAACAUCUAAACGACCUUUUCGCAGCUG UCGGACUGGAAUCGCUUCAUGACAAUUUCCGCCUUCU GGAUGGCCUGUCACCGUUUCUCUACGAUCUUGCCAAG AUAAACCCAACCGAAACGUCCCAAUGUUUCUUGGAUG UAAUCAAAGAAAAACAGGAAGAGUAUCGUAAAAAACC UCGACUGUAUCCUCAUUUGAAUAGCCUGAUUUUCCUU AAACUAGUCCCCGUAUUGUUCUCUGCAUCGGAUUUCC GCCAUCCCGUUGUAACUCCA
WD repeat-containing protein 48	AAEL021400 XM_021840350.1	CAUUAAGGGUGGAGCUGCGAUUAAAAAGUAUCACGUA CUGAACGACAAGCGGUUUAUGCUGACGAAGGACAGCG AAAUGAAUGUGGCAAUCUACGACGUUUUGAAGGUGAA GAAAGUGGAAGAUCUUGGAAAGGUGGACUACGAAGAG GAAAUCAAGAAGCGUAGCCAGAAAGUGUACGUUCCCA ACUGGUUCACGGUGGAUCUCAAAACAGGGAUGCCAAC GAUCGUUCUCGGCCAGGAUGAGGUGGACUGUUUUGCU GCAUGGGUCUCUGCCGAAGCUGGUCUUCCAGAACAUG CUGAAUCCGGAACGGAUCCGAAAGUCAACUAUGGAAG UCUGCUGUUGCAAGCCCUGUUGGAAUAUUGGAAACCU CCGCCUCCCCAUCAUCAUCUACAGGGCGUUGGUUCGG ACCUGGAUUCAAACGGAUGCGACG

CAF1C_H4-bd domain-containing protein	AAEL027479, XM_001660533.2	CGUUUAUGGUGGCUGGGACUCAAGCUGCCAGGACCCA CGUUAACAGUGUGAUCGUGAUGAAGAUGUCCAACUUG CACAGGACUUCGAAGGAACGUAAGGAUGACGAUGAUG ACUCGGAUUCGGAGUUGAGUGACGACGAGGAUGAGCA UGAGGAUAAGCGGCCACAUAUGAACUGUGCCCUCAUU AAGCACGCCGGUUGUGUGAACCGGAUUCGCGCCACGA CCUUCAACCAAUCACACUAUGUGGCCACCUGGAGCGA AAUGGGACGGGUCAACAUCUAUAACAUCAACGAUCAG UUGGCCGCAGUUGACGAUGAGCAGUCCUGCAAGAACU AUGAAACGAACAAGGUCGGGGACGGAGUGAAGCCGGA UUUU
Zinc finger protein	AAEL010847, XM_001661028.2	CCGAAGCGAUACAAACGCAGAACCAAAAUCUAUCAAU GCGAGCAGUGUGGAAAGAUCUUCCUGAACGAUGCCUU GCUAAGGCAACACGAUCUGUACCAACACAAAAAGCUC CCGGCUGCAACUUGUAAGCUUUGUGGUAAGACAUUCG CCACCAAAGCCAAUCUAGAGAAGCACUACAUUGUUCA UUCCAACGAACGGCCCUACAAGUGUGACAAAUGUUCC GCCGCCUACAAAACAUCUACCGCCCUUACAAAGCACUC GCUUCUGCACGAUAAUCUCCUGCCGUACGAGUGUCGC UACUGCGAGGAACGCUUCCUUACCCAAGGCCAAUACG CAAAACACCGUGUAUUGAACCACAACAGCCAAAUGGC GAA
PWI domain-containing protein	AAEL023022, XM_021838104.1	CCCAUCGAGUCCGAUUCCAGCGGCCACGAAGACAAUG CCGCGUUUGCAUCUCCCGAACCGGGCGCACUUAAUAA CCAUCAUGUCCACCAUGGGCACCACCCGCAGCAUGCCG GAUCGGAGACGCGGGAUUCGUUCGGGUUCGGUUCCGC CGGACCGAUGGGAAUGGGCGGCGAAGACGAAAGCUCA CGGCACUCGAUGCGGUCCAAUUCGAUGCACAGCCCCG AGGCGAACAGCAACAGCGGAAUGAACUCGCUGCUGGA GAAACACCAACCCAUUGCCCCCACGAUAUCCCUCAGCU UGAACGCAAACGCCAAGA
Aspartyl-tRNA synthetase	AAEL011655, XM_001661774.2	AGGAAGCCAUCCACGUUCUGGAGCAAAACAAAUCCAA ACUAAAGUCAGUAGUUCGGCCCGAAGAAGGCAUCAAC AAGGAGCAGGAAUUGUUCCUGGUGAGUCACUUCCAGU GCCCUCUGUUUGUAAUAGACUGGCCCAAAGCGAUCAA AUCGUUCUACAUGCGUGAGAAUCGUACUGAACCGGCC CUUGUAGACGCGAUGGAUUUCCUGGUGCCACACGUGG GCGAACUGGUUGGGGGAAGUGUCCGCGAGAAUGAAUA CGAUCGGUUGAAAGCCAAACUGCCGGAUCAGGAAGCG UUGCGAUGGUACCUGGAGCUGCGCAAGUUUGGAUCGG UCCCGAC
Aminoacyl-tRNA synthetase auxiliary protein	AAEL010514, XM_001650634.1	CUGCGAAAACAGGUGGAAGCCGCCCGGCAAAAGUUGA UCGCACUGGAAACGAAGAAUGGGAAAAAGCAGAUUUC GGUUCCGGGGCAGCAGGCUUCGGUGGACGUCAACCCG GUGGUUGUGAAGGUUGAGGCGGAGCAGGUUGUUCCAC CGAAGGCGGAAGGAGGGAAGCCUCAAAAGGACAAGAA GCCCAAGAAAGAGAAACCAGCUGCUGCGGAAGGAAAG GGGGCAGCGGCUCCUGUGGCAGCGGCCGAGGAACCUC CGAUAGACGUUGGUCG

Succinyl-CoA ligase beta subunit	AAEL011746, XM_001661816.2	CGGCAAGAUGAUCAAGCAGCUGCUGGUGACCAAGCAA ACCGGUGCUGCCGGUCGUAUUUGCAACUCGGUCAUGG UGGCCGAACGCAAAUUCCCCCGUCGUGAGUUCUACUU UGCAGUCAUGAUGGAGCGUGCAUUCAACGGUCCAGUU UUGAUUGCCUCCUCUCAGGGUGGAGUCAACAUCGAAG AGGUAGCUGCCGAAAAUCCGGAUGCCAUCGUAUACGA ACCCAUCGACAUCAAGGCCGGUUUGCAGAAGGCCCAG GCUCUGGCGAUUGCCAAGAAAGUCGGCCUGGAAGAUC ACGCCGAAGAGACAGCCAAAAUGCUGCUCAACAUGUA CGACCUUUUCGUCAAGAAGGAUGCACUGCUGAUCGAA AUCAAUCCCUAUGCCGAGGAUGCUGGAG
SEC63	AAEL025151, XM_021857125.1	AGAAUGUCAGUGCGAACCGUGCAACAAGAAACGCAUU CUGAUAUCACAUUCCGACCCGUACAAAGGCGUGAAGG CGUUCUUCGUCAAGGUGCUCAUCAUCGGUGGAUGGUU GCUGCUUGCAUUUUUGACCUACAAGGUGUCCCAAUUC GACUACGAGAUGUCCAACUUUGAUCCCUACGAGAUUC UUGGUGUACCGCUGGGAUCGUCCCAGAAGGACAUCAA GAAGGCGUACCGUACCCUAUCGGUUAUCCUGCAUCCG GAUAAGGAAACUGGUGACGAGAAGGCUUUCAUGAAGC UCACCAAGGCUUACCAAGCGCUGACUGAUGACGAAGC GCGGAAGAAUUGGGAAAAGUACGGCAAUCCGGAUGGC CCCGGAGCGACAUCGUUCGGCAUUGCUC
Glutamate synthase	AAEL014768, XM_021841419.1	GAAUUCGGAUUCAGCACGGCUCCUCUGAUUGUGAUGG GAUGCACCAUGAUGCGCAAGUGCCAUUUGAAUACCUG CCCGGUUGGUAUUGCCACCCAGGACCCAGUGCUUCGU GCCAAGUUUGCUGGAAAGCCGGAACAUGUGGUUAACU AUUUCUUCAUGCUGGCCGAAGAGAUUCGUGAAAUCAU GGCUAGUUUGGGACUGCGCAAAUUCCAAGACCUGAUC GGGCGUACCGAUUUGUUGCAAGUGCGUGAAGACCUGA CCAACAAGGCGGCUCUCCUGGAUCUGCAGAUGUUGCU CAAGAAUGCUUUGGAUCUUCGCCCA